frontiers | Frontiers in Medicine

SYSTEMATIC REVIEW
published: 12 April 2022
doi: 10.3389/fmed.2022.881551

Non-conventional and Investigational PET Radiotracers for Breast Cancer: A Systematic Review

Michele Balma[1†], Virginia Liberini[1,2†], Manuela Racca[3], Riccardo Laudicella[4,5,6], Matteo Bauckneht[7,8], Ambra Buschiazzo[1], Daniele Giovanni Nicolotti[1], Simona Peano[1], Andrea Bianchi[1], Giovanni Albano[6], Natale Quartuccio[9], Ronan Abgral[10], Silvia Daniela Morbelli[7,8], Calogero D'Alessandria[11], Enzo Terreno[12], Martin William Huellner[5], Alberto Papaleo[1] and Désirée Deandreis[2]*

[1] Nuclear Medicine Department, S. Croce e Carle Hospital, Cuneo, Italy, [2] Division of Nuclear Medicine, Department of Medical Science, University of Turin, Turin, Italy, [3] Nuclear Medicine Unit, Candiolo Cancer Institute, FPO-IRCCS, Candiolo, Italy, [4] Department of Biomedical and Dental Sciences and of Morpho-Functional Imaging, Nuclear Medicine Unit, University of Messina, Messina, Italy, [5] Department of Nuclear Medicine, University Hospital Zurich, University of Zurich, Zurich, Switzerland, [6] Nuclear Medicine Unit, Fondazione Istituto G. Giglio, Cefalù, Italy, [7] IRCCS Ospedale Policlinico San Martino, Genoa, Italy, [8] Department of Health Science (DISSAL), University of Genoa, Genoa, Italy, [9] Nuclear Medicine Unit, A.R.N.A.S. Civico di Cristina and Benfratelli Hospitals, Palermo, Italy, [10] Department of Nuclear Medicine, University Hospital of Brest, Brest, France, [11] Department of Nuclear Medicine, Klinikum Rechts der Isar TU München, Munich, Germany, [12] Department of Molecular Biotechnology and Health Sciences, Molecular & Preclinical Imaging Centers, University of Turin, Turin, Italy

OPEN ACCESS

Edited by:
Domenico Albano,
University of Brescia, Italy

Reviewed by:
Agostino Chiaravalloti,
University of Rome Tor Vergata, Italy
Ismini C. Mainta,
Geneva University Hospitals (HUG), Switzerland

***Correspondence:**
Michele Balma
mitch.balma@gmail.com

[†] These authors have contributed equally to this work and share first authorship

Specialty section:
This article was submitted to Nuclear Medicine, a section of the journal Frontiers in Medicine

Received: 22 February 2022
Accepted: 22 March 2022
Published: 12 April 2022

Citation:
Balma M, Liberini V, Racca M, Laudicella R, Bauckneht M, Buschiazzo A, Nicolotti DG, Peano S, Bianchi A, Albano G, Quartuccio N, Abgral R, Morbelli SD, D'Alessandria C, Terreno E, Huellner MW, Papaleo A and Deandreis D (2022) Non-conventional and Investigational PET Radiotracers for Breast Cancer: A Systematic Review. Front. Med. 9:881551. doi: 10.3389/fmed.2022.881551

Breast cancer is one of the most common malignancies in women, with high morbidity and mortality rates. In breast cancer, the use of novel radiopharmaceuticals in nuclear medicine can improve the accuracy of diagnosis and staging, refine surveillance strategies and accuracy in choosing personalized treatment approaches, including radioligand therapy. Nuclear medicine thus shows great promise for improving the quality of life of breast cancer patients by allowing non-invasive assessment of the diverse and complex biological processes underlying the development of breast cancer and its evolution under therapy. This review aims to describe molecular probes currently in clinical use as well as those under investigation holding great promise for personalized medicine and precision oncology in breast cancer.

Keywords: PET, breast cancer, radiotracers, molecular imaging, FES, FLT, FAPI, PSMA

INTRODUCTION

Breast cancer (BC) is a very heterogeneous disease. It is the most common malignancy in women, accounting for ∼30% of female cancers worldwide. Female BC has now an estimated 2.3 million new cases per year, representing 11.7% of all cancer cases in 2020. It is the fifth leading cause of cancer mortality worldwide, with 685,000 deaths per year. The worldwide incidence varies between 29.7 per 100,000 (transitioning countries) and 55.9 per 100,000 (transitioned countries), reflecting the association between BC incidence and the degree of economic development and associated social and lifestyle factors (1).

The disease is considered curable when it is confined to the breast or in case of spread only to axillary lymph nodes, defined as early breast cancer. Here, treatment is curative in ∼70–80% of cases, also owing to the development of new therapeutic strategies. Conversely, advanced disease

is not considered curable, but treatable, and primary goals of therapy are prolonging survival, controlling symptoms, and improving quality of life (2).

Therefore, an accurate staging of BC is critical for its clinical and therapeutic management. In clinical practice, ultrasonography, mammography, and magnetic resonance imaging (MRI) are mainly used to assess the local disease extent. In order to assess the presence of distant metastases, whole-body imaging is required. Although radiological imaging, such as computed tomography (CT) and MRI, is still more widely used for this purpose, in recent years nuclear medicine imaging has also gained more importance, thanks to the use of positron emission tomography (PET), PET/CT or PET/MRI. In particular, 2-deoxy-2-[^{18}F]fluoro-D-glucose ([^{18}F]F-FDG) PET is helpful in identifying otherwise undetected distant metastases in advanced BC (3–5). However, several factors can result in false-negative [^{18}F]F-FDG imaging in BC, owing, e.g., to the small size of a tumor or to its molecular and histological characteristics (6).

Abbreviations: [^{11}C]C-choline, N-[^{11}C]methyl-choline; [^{11}C]C-MET, L-methyl-[^{11}C]-methionine; [^{18}F]F-FACBC, anti-1-amino-3-[^{18}F]-fluorocyclobutane-1-carboxylic acid; [^{18}F]F-FASu, [^{18}F]-5-fluoro-aminosuberic acid; [^{18}F]F-FAZA, [^{18}F]-fluoroazomycin-arabinoside; [^{18}F]F-FDG, 2-deoxy-2-[^{18}F]fluoro-D-glucose; [^{18}F]F-FENP, 21-fluoro-16α-ethyl-19-norprogeserone; [^{18}F]F-FES, 16α-[^{18}F]-fluoro-17β-estradiol; [^{18}F]F-FETE, 1-(-2(-2(-2[^{18}F]fluoroethoxy)ethoxy)ethyl)-1H-1,2,3-triazole-estradiol; [^{18}F]F-FETNIM, [^{18}F]-fluoroerythronitroimidazole; [^{18}F]F-FFNP, 21-^{18}F-fluoro-16α,17α-[(R)-(1′-α-furylmethylidene)dioxy]-19-norpregn-4-ene-3, 20-dione; [^{18}F]F-FGln, [^{18}F]-(2S, 4R)4-fluoroglutamine; [^{18}F]F-FLT, [^{18}F]-fluoro-3′-deoxy-3′-L-fluorothymidine; [^{18}F]F-FMISO, [^{18}F]fluoromisonidazole; [^{18}F]F-FSPG, (4S)-4-(3-[^{18}F]-fluoropropyl)-l-glutamate; [^{18}F]F-HX4, [^{18}F]-3-fluoro-2-(4-((2-nitro-1H-imidazol-1-yl)methyl)-1H-1,2,3-triazol-1-yl)propan-1-ol; [^{18}F]F-ISO-1, N-(4-(6,7-dimethoxy-3,4-dihydroisoquinoline-2(1H)-yl)butyl)-2-(2-[^{18}F]-fluoroethoxy)-5-methylbenzamide; [^{18}F]F-RP-170, [^{18}F]-1-(2-1-(1H-methyl) ethoxy)-methyl-2-nitroimidazole; 4FM-[^{18}F]F-FES, 4-fluoro-11β-methoxy-16α-[^{18}F]-fluoroestradiol; ABCB1, multidrug resistance protein 1; BBN, bombesin receptor; BC, breast cancer; BRCA1, breast cancer gene 1; BRCA2, breast cancer gene 2; CAF, cancer associated fibroblasts; CAP, college of american pathologists; CT, computer tomography; CTLA-4, cytotoxic T-lymphocyte–associated protein 4; Cu-ATSM, non-nitroimidazole compound copper(II)diacetyl-bisN(4)-methylthiosemicarbazone; DCIS, ductal carcinoma *in situ*; EGFR, epidermal growth factor receptor; ENT1, equilibrative nucleoside transporter 1; ER, estrogen receptor; FAPα, fibroblast activation protein-α; FDA, food and drug administration; FMAU, 1-(29-deoxy-29-fluoro-b-D-arabinofuranosyl) thymine; GLUTs, glucose transporters; GRP, gastrin releasing peptide; GRPR, gastrin releasing peptide receptor; HER2, human epidermal growth factor receptor 2; HIF-1, hypoxia inducible factor 1; IBC, invasive breast cancer; IBC-NST, invasive breast cancer of no special type; ICIs, immune checkpoint inhibitors; ICOS, inducible T-cell costimulator; IDC, invasive ductal carcinoma; IHC, immunohistochemistry; ILBC, invasive lobular breast carcinoma; ISH, *in situ* hybridization; LHRH, luteinizing hormone-releasing hormone; ML-10, 2-(5-fluoro-pentyl)-2- methyl-malonic acid; MRI, magnetic resonance imaging; NAC, neoadjuvant chemotherapy; NE BCs, neuroendocrine differentiation breast cancers; NSCLC, non-small cell lung cancer; OS, overall survival; PCa, prostate cancer; PD-1, programmed cell death protein 1; PD-L1, programmed cell death ligand 1; PET, positron emission tomography; PFS, progression free survival; Pgp, P-glycoprotein; PR, progesterone receptor; PRRT, peptide receptor radionuclide therapy; PSMA, prostate specific membrane antigen; RGD, arginine-glycine-aspartic acid; SBR, scarff-bloom-richardson; SSTR, somatostatin receptors; SUV, standardized uptake value; TBR, tumor-to-background ratio; TILs, tumor-infiltrating lymphocytes; TK-1, thymidine kinase-1; TK-2, thymidine kinase-2; TME, tumor microenvironment; TNBC, triple negative breast cancer; VEGF, vascular endothelial growth factor; WHO, world health organization.

BREAST CANCER BIOLOGY AND CLASSIFICATION

Regarding BC biology and classification, invasive breast cancer (IBC) encompasses a broad spectrum of histological subtypes, with the World Health Organization (WHO) recognizing at least 18 histologically different varieties. Invasive breast cancer of no special type (IBC-NST), previously known as invasive ductal carcinoma, is the most frequent subgroup, accounting for 40–80% of cases. The second most common histological subtype is invasive lobular breast carcinoma (ILBC) (7).

In recent years, the advancement and widespread application of "omics" technologies (genomics, epigenomics, transcriptomics, or proteomics, among others) has led to new discoveries based mainly on morphological and immunohistochemical characterization of the tumor, but also on genetic profiling of the tumor. In 10% of BC cases, there is a genetic predisposition and the most commonly associated germline mutations are *breast cancer gene 1* (BRCA1) and *breast cancer gene 2* (BRCA2) (8).

The most important biomarkers of BC are estrogen receptor (ER), progesterone receptor (PR), Ki-67 and human epidermal growth factor receptor 2 (HER2) status. The ErbB2/HER2 gene is a proto-oncogene located in the long arm of chromosome 17 (17q21–q22), implicated in the production of the transmembrane protein HER2, a membrane receptor protein of the tyrosine kinase type, located on the outer cell surface and leading to cell growth and differentiation (9). According to the College of American Pathologists (CAP), these are the only validated biomarkers to predict therapy response, together with patient age, histological grade, histological subtypes and TNM status [tumor size (T), lymph node status (N), and presence of distant metastases (M)] (7).

Indeed, their evaluation is also fundamental for subtype classification. Among different classifications, the most widely used one is the intrinsic classification by Perou and Sorlie, which identifies four subtypes of BC, based on a 50-gene expression signature (PAM50): luminal A and luminal B (expressing ER), basal-like, and HER2-enriched (without ER expression) (10). The first subtype, Luminal A BC, is characterized by ER+ and/or PR+, and HER2- configuration. It accounts for ∼50–60% of BC cases and is associated with a comparably good prognosis. The second subtype, Luminal B BC, is characterized by an ER+ and/or PR+ (but lower than Luminal A), and HER2+ (Luminal B-like HER2+) or HER2- (Luminal B-like HER2-) arrangement. It accounts for ∼30% of cases and may be associated with a higher Ki-67 value and a poorer prognosis (11). Approximately 10% of BC cases are represented by the HER2-enriched subtype, which is characterized by ER-, PR-, and HER2+ setting and an even poorer prognosis (12). The fourth subtype of BC is represented by basal-like/triple-negative breast cancer (TNBC), characterized by an ER-, PR-, and HER2- arrangement. This subtype, often occurring in younger women, constitutes ∼15–20% of BC and is associated with a higher aggressiveness and a worse prognosis than the other molecular subtypes of BC (13).

Currently, a classification of five surrogate intrinsic subtypes is more commonly used in clinical practice; this classification is based on the assessment of ER, PR, HER2, and the proliferation marker Ki-67 (14). The histologic and molecular features of breast cancer are summarized in **Figure 1**.

The treatment choice depends on the molecular and histological characteristics of the tumor and therefore it is important to consider these biomarkers for their therapeutic implications. In particular, HER2 protein overexpression represents a negative prognostic factor, being more commonly found in cases of high-grade tumors and in the presence of lymph node metastases. It is associated with a high mortality rate (9). Moreover, it has been demonstrated that hormone receptor positive tumors show a response to hormone therapy and usually have a more indolent course: hormone treatment often represents the first-line therapy in metastatic BC expressing hormone receptors (2, 8, 11). However, there are fundamental limitations for proper patient assessment. First, it is not always possible to identify the receptor status of the disease, especially in metastatic patients with lesions difficult to biopsy. Second, it must be remembered that the receptor status of secondary lesions may be different from the one of the primary tumor. Third, an invasive assessment of the receptor status for every new appearing lesion is not feasible.

In recent years, nuclear medical imaging (particularly receptor-specific imaging) has played an increasingly important and intriguing role through the development of new probes, capable of overcoming the limitations of *in-vitro* assessment (based on invasive tests and multiple biopsies), non-invasively obtaining different tumor characteristics *in-vivo*, which are crucial for optimal and personalized treatment.

Here, we will review several PET probes already used in clinical practice for BC and several promising radiopharmaceuticals currently under investigation for further use in this field (as shown in **Figure 2**), with the aim of analyzing their advantages and limitations and possible future developments.

MATERIALS AND METHODS

We searched the PubMed, PMC, Scopus, Google Scholar, Embase, Web of Science, and Cochrane library databases (between January 1990 and December 2021), using the following both as text and as MeSH terms: ("breast neoplasm*" OR "breast" OR "breast cancer*") AND ("PET" OR "positron emission tomography" OR "PET/CT" OR "PET/MR") AND ("FDG" OR "MET" OR "FLT" OR "FMISO" OR "FES" OR "estradiol" OR "trastuzumab" OR "PD-L1" OR "PSMA" OR "FAPI" OR "FACBC" OR "flucicovine" OR "FAZA" OR "GRPR" OR "DOTATOC" OR "DOTATATE"). No language restriction was applied to the search, but only articles in English were reviewed.

The systematic literature search returned 1,123 articles. Additional filters, such as original article and/or research article, and study including only humans and with 10 or more subjects, were used. Reviews, clinical reports, meeting abstracts, and editorial comments were excluded. Due to the comparably high number of studies available on this topic, an additional exclusion was based on citation threshold >20 citations for years 2010–2019 and >10 citation for 2020. According to the PRISMA flow-chart (15), after duplicate removal, 175 articles have been considered, fully read, analyzed, and extensively described according to their title and abstract. Relevant studies that were not obtained by the original search were included through cross-references; most relevant reviews on this topic were also reported.

MOLECULAR IMAGING OF GLYCOLYSIS

2-[^{18}F]-Fluoro-2-Deoxy-D-Glucose ([^{18}F]F-FDG)

To date, 2-[^{18}F]-fluoro-2-deoxy-D-glucose ([^{18}F]F-FDG) represents the most widely used radiopharmaceutical for PET imaging of BC patients. Glucose metabolism in BC cells is increased compared with normal tissues due to increased glycolysis, a phenomenon known as Warburg effect. [^{18}F]F-FDG is an excellent biomarker of metabolism resembling glucose, which is entering into neoplastic cells, characterized by an increased number of glucose membrane transporters (GLUTs). Once intra-cellularly, [^{18}F]F-FDG is then phosphorylated by hexokinase into [^{18}F]F-FDG-6-phosphate, but unlike glucose, [^{18}F]F-FDG-6-phosphate is very slowly metabolized further and thus remains trapped in the cell (16).

Current evidence does not support the use of [^{18}F]F-FDG PET/CT in the staging of locoregional-limited disease, although it may be useful when conventional methods are inconclusive (3). In contrast, [^{18}F]F-FDG PET/CT is recommended for initial staging in patients with clinical stage ≥ IIB BC (preferably performed before surgery), and it may also be used for staging patients with clinical stage IIA BC (T1N1 or T2N0), again preferably performed before surgery. [^{18}F]F-FDG PET/CT is also recommended in cases of suspected or known BC recurrence, for early assessment of response to neoadjuvant therapy (particularly in TNBC or HER2+ disease) and for assessment of response to systemic treatment of metastatic BC (particularly for bone metastases) (4, 5). Indeed, [^{18}F]F-FDG PET/(CT or MRI) has shown high sensitivity for detecting locoregional and distant metastases both in staging and restaging setting, showing high prognostic value. A recent systematic review and meta-analysis by Han et al. (17) showed that [^{18}F]F-FDG PET/CT significantly changes the initial staging in newly diagnosed BC patients, with a relevant impact on patient management: the pooled proportions of changes in stage and management were 25% [95% confidence interval (CI), 21–30%] and 18% (95% CI, 14–23%), respectively.

However, it is necessary to account for potential limitations of [^{18}F]F-FDG PET/CT examinations in order to provide an appropriate interpretation: from the small tumor size (because of the low spatial resolution of PET tomographs and the partial volume effect) to the low sensitivity for specific histological subtypes with low [^{18}F]F-FDG avidity. Invasive ductal carcinoma (IDC) shows higher [^{18}F]F-FDG uptake than both ILBC and ductal carcinoma *in situ* (DCIS), as shown in **Figure 3**, making

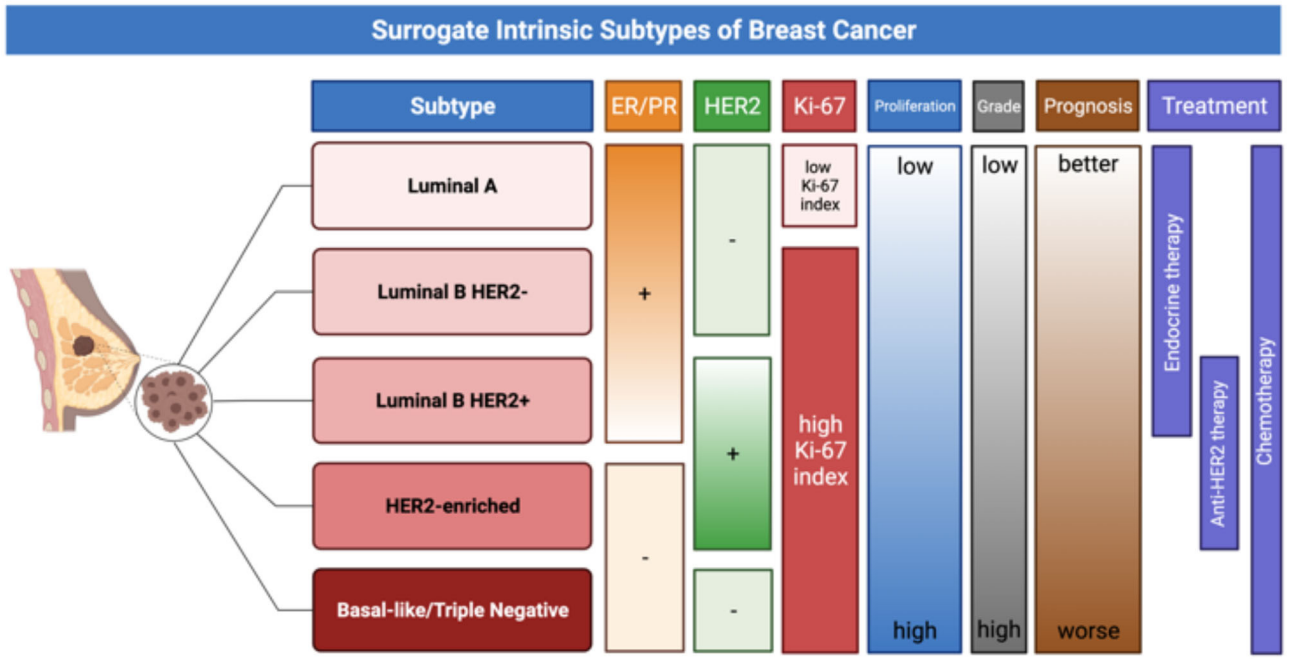

FIGURE 1 | The figure provides a schematic representation of surrogate intrinsic BC subtypes (14), based on histologic and molecular features, which have significant implication for prognosis and treatment choice.

[^{18}F]F-FDG PET/CT more effective in staging invasive ductal carcinoma (18).

[^{18}F]F-FDG uptake may also vary depending on the receptor status of a lesion: lower uptake is observed in well-differentiated tumors (ER-positive and PR-positive) compared to ER-negative and PR-negative tumors. Several studies have shown that the standardized uptake value (SUV) is substantially higher in the TNBC subtype. Among luminal tumors, however, [^{18}F]F-FDG uptake is lower in luminal A than in luminal B subtype (19–21). In general, higher [^{18}F]F-FDG uptake is associated with a worse prognosis, as in cases of grade 3 tumors compared to grade 1 and 2 tumors (according to the Elston-Ellis modification of the Scarff-Bloom-Richardson (SBR) classification system), in tumors with increased proliferation (as assessed by the Ki67 index) and in tumors with mutated p53 (22). It should be remembered that [^{18}F]F-FDG is not a specific radiotracer for BC or malignancy in general, and numerous conditions may lead to false-positive results, such as infection, fibroadenoma, ductal adenoma, inflammatory granulomatous mastitis, and fibrocystic changes (23–28). Some authors investigated the use of late imaging to improve specificity, since uptake usually increases on delayed images in case of malignancy, while it often decreases in inflammatory lesions (29, 30). However, [^{18}F]F-FDG can only provide information on cellular metabolism and not on other tumor characteristics, such as proliferation and receptor status. Hence several other radiopharmaceuticals have been developed with the aim to assess other more specific features of BC lesions, overcoming the limitations of [^{18}F]F-FDG.

MOLECULAR IMAGING OF AMINO ACID TRANSPORTER, CELLULAR PROLIFERATION AND HYPOXIA

Amino Acid Transporter

In BC, as well as in other malignancies, increased protein synthesis has been observed associated with increased amino acid consumption and overexpression of amino acid transporters in the cell membrane (31).

L-methyl-[^{11}C]-methionine ([^{11}C]C-MET) represents one of the first radiolabeled amino acids used for the assessment of amino acid metabolism in oncologic PET imaging (32), in one of the first studies on the use of [^{11}C]C-MET in BC patients by Leskinen-Kallio et al., both the primary tumor and metastases could be visualized, with a correlation between [^{11}C]C-MET uptake and the fraction of cells in mitosis (S phase) in these lesions, indicating that [^{11}C]C-MET uptake may be related to the proliferation rate of BC.

Subsequent studies focused on assessing treatment response in BC, demonstrating that [^{11}C]C-MET uptake was reduced in responsive lesions, while it was unchanged or even increased in patients with progressing disease (33, 34). In particular, a reduction in [^{11}C]C-MET uptake at the level of BC lesions can also occur early after the first treatment cycle (chemotherapy or hormone therapy), before objective clinical response or reduction in lesion size, thereby potentially allowing for an early discrimination between responding and non-responding patients (35).

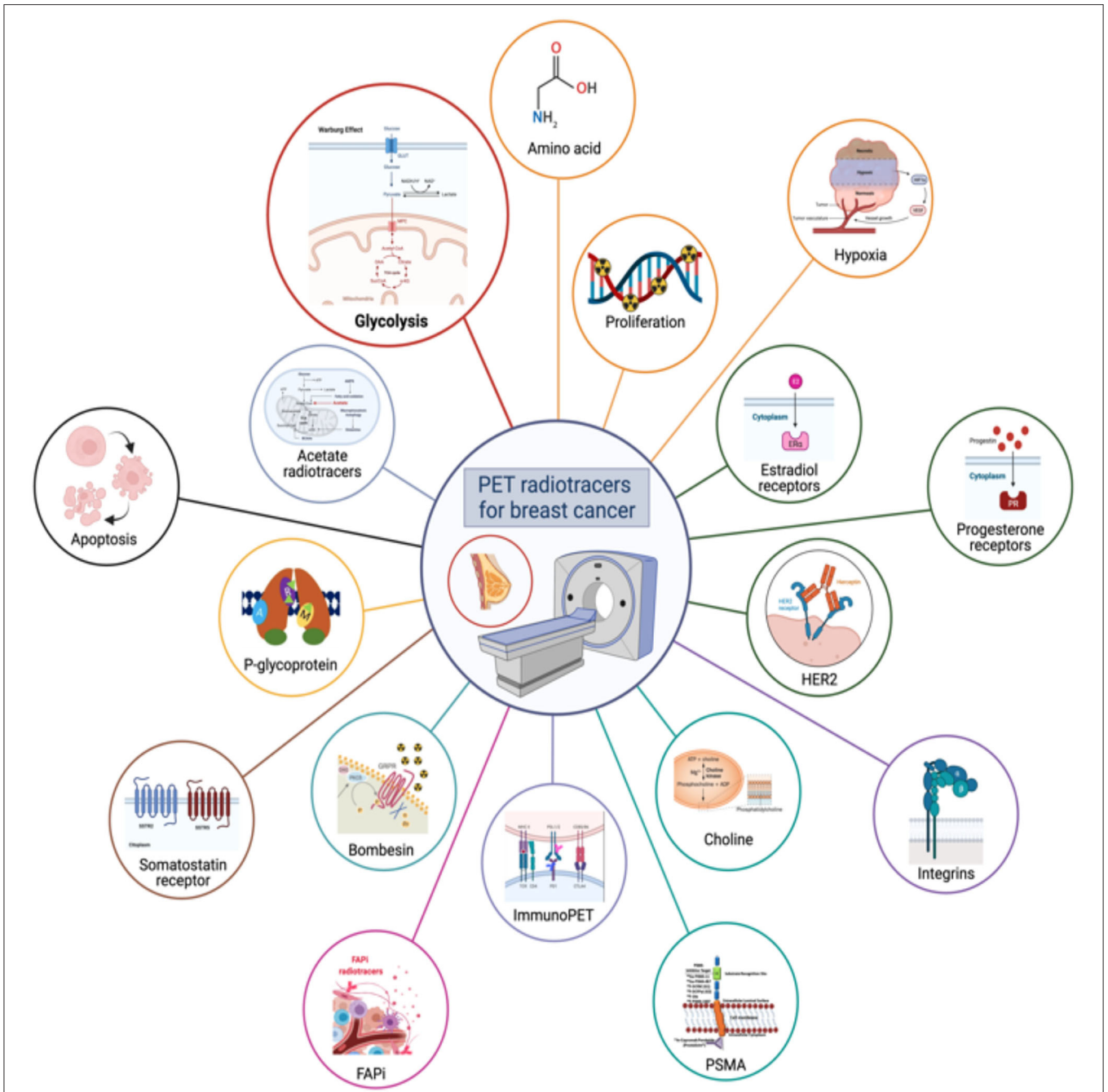

FIGURE 2 | The figure shows a schematic representation of all major radiotracers currently in clinical use in BC or under evaluation.

In the literature, few studies with small sample size directly compared [^{18}F]F-FDG PET/CT and [^{11}C]C-MET PET/CT treatment response assessment in BC patients. Although [^{11}C]C-MET was favored in some individual cases (36), in the majority of cases substantially overlapping results in terms of efficacy were obtained with these two radiotracers, both showing low diagnostic value in small lesions (37). [^{11}C]C-MET and other amino acid radiotracers, such as 6-[^{18}F]F-fluoro-l-dopa ([^{18}F]-FDOPA), are particularly useful for the detection of brain metastases, to distinguish recurrent or progressive brain metastases (RPBM) from late or delayed radiation injury (LDRI) and also for the differential diagnosis with other pseudo-tumoral lesions, such as tumefactive multiple sclerosis (TMS) or brain abscesses, as demonstrated in the **Figure 4** (38–40).

The main limitations of [^{11}C]C-MET are: (1) a potential suboptimal evaluation of metastatic lesions in the liver and bone

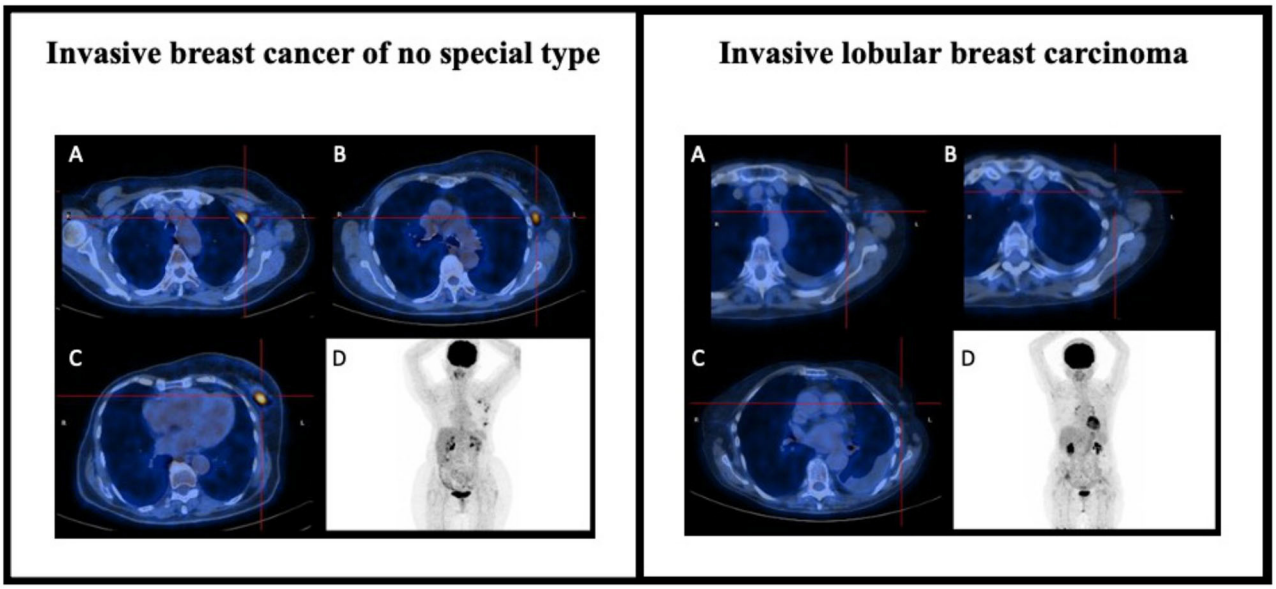

FIGURE 3 | [^{18}F]F-FDG PET/CT in BC staging. On the left, the case of an 83-year-old lady with previous *in situ* BC on the right and suspected recurrence of breast cancer on the left. Staging [^{18}F]F-FDG PET/CT scan showed focal and elevated uptake at the level of the breast lesion on the left upper-external quadrant **(C)** and at the level of several ipsilateral axillary lymph nodes suspected for secondary localization of disease **(A,B)**, as also shown in the MIP images **(D)**. The cytologic finding was consistent with the clinical suspicion of IBC-NST recurrence (ER 98%, PR 99%, anti-Ki67 23%, anti c-erbB2 negative). On the right, the case of a 72-year-old lady hospitalized for dyspnea and CT findings of right pleural effusion concomitant to left mammary nodule and mediastinal lymphadenopathies. Staging PET scans did not show any FDG uptake in the suspicious lesions reported on CT scan, either in the breast **(C)** or in the ipsilateral axillary lymph nodes **(A,B)**, as also shown in MIP images **(D)**. The cytological findings were consistent with the clinical suspicion of ILBC (ER 78%, PR 55%, anti-Ki67 46%, anti c-erbB2 negative).

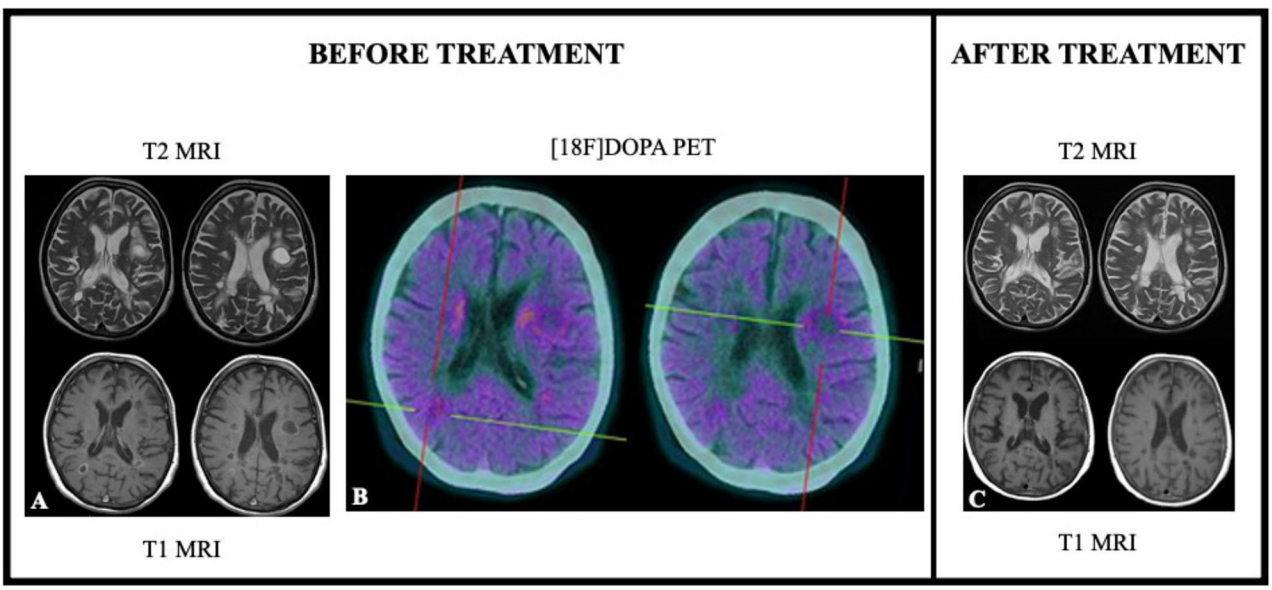

FIGURE 4 | [^{18}F]F-DOPA PET and MRI results in a case of differential diagnosis between tumefactive plaque due to multiple sclerosis and brain metastasis from breast cancer. Seventy-one years old female patient previously treated for BC. ceMRI showed the presence of at least two hyperintense at T2 sequences **(A)** and hypointense at T1 sequences **(A)** (the largest in left frontal lobe). [^{18}F]F-DOPA PET/CT showed a very mild tracer uptake supporting the hypothesis of tumefactive lesion due to multiple sclerosis **(B)**. ceMRI performed 3 months after therapy administration showed reduction in both lesion size and contrast enhancement **(C)**.

marrow, due to the high physiological tracer uptake in these organs (2, 41) the short half-life of only 20 min of [^{11}C], limiting its use to centers with an on-site cyclotron; (3) the presence of non-protein metabolites, that may reduce the image quality.

Because of these limitations, other [^{18}F]-labeled amino acids have been developed. Anti-1-amino-3-[^{18}F]-fluorocyclo-butane-1-carboxylic acid ([^{18}F]-fluciclovine or [^{18}F]F-FACBC) is a synthetic amino acid, a leucine analog, mainly used in patients with prostate cancer, particularly in cases of biochemical disease recurrence (42–44).

Studies have shown that uptake of [^{18}F]F-FACBC is higher in BC than in benign lesions and healthy breast tissue, with higher uptake in patients with higher tumor grade. This radiotracer is also suitable for the detection of metastasis (such as bone, lung, brain, and lymph node metastases). Interestingly, two different studies showed that [^{18}F]F-FACBC avidity is higher than [^{18}F]F-FDG avidity in ILBC and equal to [^{18}F]F-FDG avidity in IDC (45, 46). Furthermore, Ulaner et al. observed not only that primary ILCs (4/14) have higher [^{18}F]F-FACBC avidity than [^{18}F]F-FDG avidity (median SUVmax 6.1 vs. 3.7, respectively), but also that primary IDCs have an inverse relationship, with lower [^{18}F]F-FACBC avidity than [^{18}F]FDG avidity (median SUVmax 6.8 vs. 10.0, respectively) (45).

[^{18}F]F-FACBC PET/CT has also been used to assess response to neoadjuvant chemotherapy in patients with advanced BC. Ulaner et al. observed that changes in [^{18}F]F-FACBC uptake correlated with pathological tumor response (47). However, [^{18}F]F-FACBC is characterized by physiological high hepatic uptake and this represents a limitation for the detection of secondary lesions in the liver, a common site of BC metastases (46).

Hence, other amino acid metabolism radiotracers were developed. Two different radiotracers address the x_c^- transporter, which mediates cellular uptake of cysteine by exchanging glutamate. The radiotracer (4S)-4-(3-[^{18}F]-fluoropropyl)-l-glutamate ([^{18}F]F-FSPG) was evaluated by Baek et al. in 5 BC patients. They demonstrated that [^{18}F]F-FSPG uptake may vary between different histological or molecular subtypes, however, detecting only 30 of 73 BC lesions with known [^{18}F]F-FDG avidity (48). Similar results were also obtained by studies on [^{18}F]-5-fluoro-aminosuberic acid ([^{18}F]F-FASu), which might have higher sensitivity than [^{18}F]F-FDG for some tumor subtypes of BC (49, 50). However, the use of both tracers today is limited to a research setting.

Finally, other two interesting radiotracers are [^{11}C]C-labeled tyrosine (L-[1-^{11}C]C-tyrosine), which appears to be more accurate than [^{18}F]F-FDG in differentiating malignant from benign lesions (51), and [^{18}F]-(2S, 4R)4-fluoroglutamine ([^{18}F]F-FGln), which has been recently used in the assessment of glutamine pool changes in patients with TNBC (52).

Cellular Proliferation

One of the characteristic biological feature of malignant tumors is their increase in cell proliferation, which is correlated with tumor aggressiveness (53).

Thymidine is the only nucleotide incorporated into DNA but not RNA, making it an attractive target for the development of novel radiotracers that may allow for an assessment of DNA synthesis through the thymidine salvage pathway (54). One of the first cell proliferation probes developed was [^{11}C]C-thymidine, which was rapidly discarded in favor of new [^{18}F]-labeled probes due to the short half-life of [^{11}C], demanding radiochemistry, and complicated pattern analysis (55–59).

Second-generation [^{18}F]-labeled probes have been developed to overcome these limitations. Today, the most widely one used is [^{18}F]-fluoro-3′-deoxy-3′-L-fluorothymidine ([^{18}F]F-FLT). [^{18}F]F-FLT enters cells by passive diffusion and *via* the equilibrative nucleoside transporter 1 (ENT1), and is then phosphorylated by thymidine kinase-1 (TK-1), but cannot participate further in DNA synthesis and remains trapped intracellularly. Although this radiopharmaceutical is not used in clinical routine, some studies have shown that [^{18}F]F-FLT can detect BC lesions, both primary and secondary ones (54, 60). In particular, a strong correlation between [^{18}F]F-FLT uptake (in terms of SUV) and the standard immunohistochemical marker of proliferation, Ki-67, has been observed (61, 62).

Despite this correlation, there are some limitations that need to be taken into account, such as the lower uptake gradient of [^{18}F]F-FLT compared to [^{18}F]F-FDG into BC lesions (with potential false negative results) and its high uptake into liver and bone marrow (with potential disadvantages for lesion detection in these organs) (54, 63). Although [^{18}F]F-FLT is absorbed to a lesser extent than [^{18}F]F-FDG in inflammatory tissue, leading to less false positives (64), the use of [^{18}F]F-FLT PET/CT for staging has been discouraged by these issues.

Further studies have also evaluated the role of this radiotracer in assessing treatment response. Pio et al. showed that [^{18}F]F-FLT uptake could predict changes in tumor proliferation after a cycle of cytotoxic chemotherapy (65). Kenny et al. observed an early reduction of [^{18}F]F-FLT uptake into BC lesions, as an expression of change in cell proliferation, as early as 1 week after chemotherapy, and before an appreciable reduction in lesion size on CT (66). In 2021, López-Vega et al. evaluated, in a prospective phase II study, the accuracy of [^{18}F]F-FLT PET/CT for the detection of proliferative status in 70 patients with primary stage II/III BC at baseline, during bevacizumab treatment (cycle 1; C1), and after four cycles of neoadjuvant docetaxel doxorubicin and bevacizumab every 3 weeks (C2–C5). They observed a significant decrease in tumor proliferation as measured by [^{18}F]F-FLT uptake during C1 ($p \leq 0.001$) compared to baseline, independent of tumor subtype (67).

However, in two recent different studies, [^{18}F]F-FLT PET/CT did not show an advantage over [^{18}F]F-FDG PET/CT in predicting treatment response and survival in patients with metastatic BC. In one study, Romine et al. evaluated the ability of these two radiotracers to measure early response to endocrine therapy from baseline until surgical resection in two separate cohorts of women with early stage ER+ BC: 22 patients underwent two sequential [^{18}F]F-FDG scans and 27 patients underwent two sequential [^{18}F]F-FLT scans, thereof the first scan prior to endocrine therapy and the second one pre-operatively. Pre- and post-therapy PET measures showed strong rank-order agreement with Ki-67 percentages for both

radiotracers, demonstrating no concrete advantage in using [^{18}F]F-FLT instead of [^{18}F]F-FDG (68). In another prospective study, Su et al. aimed to compare the value of interim [^{18}F]F-FLT and [^{18}F]F-FDG PET/CT to predict treatment outcome in 25 patients with metastatic BC after salvage therapy. All patients had dual radiotracer PET/CT at baseline, and after the 1st and 2nd cycle of systemic chemotherapy. Metabolic response determined by Response Criteria in Solid Tumors (PERCIST) on interim [^{18}F]F-FDG PET/CT after 2 cycles showed a high accuracy in predicting clinical response (AUC = 0.801, $p = 0.011$), with significantly higher 2-year progression free survival (PFS) for responders (53.8 vs. 16.7%, respectively, $p = 0.014$) and higher 2-year overall survival (OS) (100 vs. 47.6%, respectively, $p = 0.046$) compared with non-responders. In contrast, survival differences between responders and non-responders at interim [^{18}F]F-FLT PET/CT were not significant (69).

The 1-(29-deoxy-29-fluoro-b-D-arabinofuranosyl) thymine ([^{18}F]F-FMAU) is another [^{18}F]-labeled thymidine analog used for PET imaging. Also for this new probe, the few available studies have low patient numbers. Despite this limitation, Sun et al. observed a good tumor to healthy tissue ratio (average BC SUVmax of 2.17), low uptake at the bone marrow level, but high physiological uptake at the hepatic level (70). Moreover, a 5–10 times lower uptake of [^{18}F]F-FMAU was observed in more aggressive tumors, such as TNBC, compared to [^{18}F]F-FLT, probably because [^{18}F]F-FMAU is a substrate of the mitochondrial enzyme thymidine kinase-2 (TK-2) with low specificity for TK-1 (71).

New proliferation probes, such as [^{18}F]-benzamide analogs, that bind to sigma 2 (s2) receptors, are under development. The function of these receptors appears to be associated with the potassium and calcium ion channel transport (72). From this radiotracer category, the N-(4-(6,7-dimethoxy-3,4-dihydroisoquinoline-2(1H)-yl)butyl)-2-(2-[^{18}F]-fluoroethoxy)-5-methylbenzamide ([^{18}F]F-ISO-1) was the first one to be evaluated in a clinical study with 30 cancer patients (13/30 with proven BC). The study observed a correlation between tumor uptake and ki-67. However, also this radiotracer showed high uptake in the liver and pancreas, which may limit its use in BC patients (73). Finally, McDonald et al. reported the results of a prospective clinical trial (NCT02284919) dedicated to [^{18}F]F-ISO-1 PET/CT in 28 women with 29 primary invasive BC. Tumors stratified into the high Ki-67 group (≥20%) had higher SUVmax than the low Ki-67 group (<20%) ($p = 0.02$). SUVmax showed a positive correlation with Ki-67 in all breast cancer subtypes ($\rho = 0.46$, $p = 0.01$) and SUVmax corrected for partial volume was positively correlated with Ki-67 in invasive ductal carcinoma ($\rho = 0.51$, $p = 0.02$). The study also showed that the uptake of [^{18}F]F-ISO-1 in breast cancer correlates modestly with the *in-vitro* Ki-67, obtained by biopsy (74).

Hypoxia

Hypoxia in cancer lesions occurs when there is an imbalance between increased cellular metabolism and insufficient oxygen (O2) supply; characterized by high O2 consumption, a disorganized tumor vasculature with slow blood flow and consequent low arteriolar supply to cancer cells. These phenomena are associated with an overexpression of hypoxia-inducible factor 1 (HIF)-1 and increased glycolysis, angiogenesis and resistance to apoptosis (75).

The presence of hypoxia in many tumor types, including BC, has been shown to induce resistance to both chemotherapy and radiation therapy, representing a negative prognostic factor (76).

Radiolabeled nitroimidazoles represent the most widely developed radiopharmaceuticals for PET imaging of hypoxia in oncology. Among these, [^{18}F]fluoromisonidazole ([^{18}F]F-FMISO) is the one most widely used (77). Owing to its lipophilic nature, it diffuses through cell membranes, is then reduced by nitroreductases in vital cells (when tissue pO2 is <10 mmHg) and remains trapped within the cells. At 2–4 h after administration, retention is considered specific for cellular hypoxia (78).

Although many with [^{18}F]F-FMISO PET/CT studies have been conducted in other types of cancer (79), only a few studies covered [^{18}F]F-FMISO PET/CT in BC. In a study of Rajendran et al. on four different tumor types, including seven BC patients, glucose metabolism ([^{18}F]F-FDG PET/CT) and hypoxia ([^{18}F]F-FMISO PET/CT) were directly compared. They reported a discordance between the uptake of these two radiotracers, which might be tumor-type-specific: the mean correlation coefficients between [^{18}F]F-FMISO and [^{18}F]F-FDG SUV-uptake were 0.47 for BC. The linear association between [^{18}F]F-FMISO and [^{18}F]F-FDG varied among the tumor types examined, with the order sarcoma < brain < breast < head and neck. The differences between average correlations within the tumor types were highly significant ($p < 0.005$) (80). Chen et al. used [^{18}F]F-FMISO in patients with ER-positive stage II-IV BC both before and after 3 months of aromatase inhibitor therapy, showing the ability of this method to predict resistance to endocrine therapy (81). In the aforementioned prospective phase II study by López-Vega et al., the 70 patients with primary stage II/III BC were evaluated not only with [^{18}F]F-FLT, but also with [^{18}F]F-FMISO PET/CT during bevacizumab treatment. Interestingly, [^{18}F]FMISO SUVmax at baseline was modestly correlated with VEGFR-2 expression ($\rho = 0.26$, $p = 0.02$), even if [^{18}F]F-FMISO uptake did not differ significantly before or after bevacizumab therapy or by BC subtype (67).

The main disadvantages of [^{18}F]F-FMISO are a slow clearance from blood and healthy tissue (resulting in a reduced target/background ratio), its relatively short half-life (110 min), and the need for imaging acquisitions at 2–3 h after administration. Therefore, second-generation compounds have been developed that offer a better target/background ratio and have better pharmacokinetic properties. Among these new probes is [^{18}F]-fluoroazomycin-arabinoside ([^{18}F]F-FAZA), which is more hydrophilic than [^{18}F]F-FMISO and shows better clearance kinetics, with a more favorable target/background ratio (82).

Other hypoxia probes for PET imaging already studied in varies tumor type, but not yet in BC, include: -the more lipophilic [^{18}F]-2-nitroimidazol-pentafluoropropyl acetamide (83); -the non-nitroimidazole compound copper(II)diacetyl-bisN(4)-methylthiosemicarbazone (Cu-ATSM), which can be

labeled with either [^{60}Cu] or [^{64}Cu] (84–87); -the [^{18}F]-fluoroerythronitroimidazole ([^{18}F]F-FETNIM) (88); -the [^{18}F]-1-(2-1-(1H-methyl)ethoxy)-methyl-2nitroimidazole ([^{18}F]F-RP-170) (89); -the [^{18}F]-3-fluoro-2-(4-((2-nitro-1H-imidazol-1-yl)methyl)-1H-1,2,3-triazol-1-yl)propan-1-ol ([^{18}F]F-HX4) (90).

MOLECULAR IMAGING OF RECEPTORS

Estradiol Receptor

Being aware of the receptor status of BC lesions is essential not only for a correct characterization of the disease from an anatomical and pathological point of view, but also for defining eligibility for endocrine therapy targeting steroid receptors, which represents one of the most effective systemic treatments. As already mentioned, the histological and molecular classification of BC is mainly based on the expression of ER, PR, HER2, and the proliferation marker Ki-67. ER- or PR-positive BCs are usually characterized by lower aggressiveness and better prognosis than HER2-enriched and triple-negative subtypes (12, 13). However, the receptor status of the disease is not always easily identifiable, especially in metastatic patients where secondary lesions may have receptor status different to the primary tumor (91).

[^{18}F]-labeled receptor ligands have gained importance over the years, allowing for an *in-vivo* assessment of the receptor status both in the primary tumor and in metastatic lesions, such as [^{18}F]-labeled estradiol (especially endogenous estradiol, E2) for ER imaging (especially ERα) (92, 93).

16α-[^{18}F]-fluoro-17β-estradiol ([^{18}F]F-FES) is an analog of E2, with an affinity for ERα slightly higher than that of E2 (94), and with a similar biodistribution. It is metabolized in the liver and excreted through the biliary tract and then reabsorbed through the small intestine (it does not accumulate physiologically in the large intestine) and is then eliminated mainly through the urine (only 5% in the feces) (95–97). An example of [^{18}F]F-FES PET/CT scan is shown in **Figure 5**.

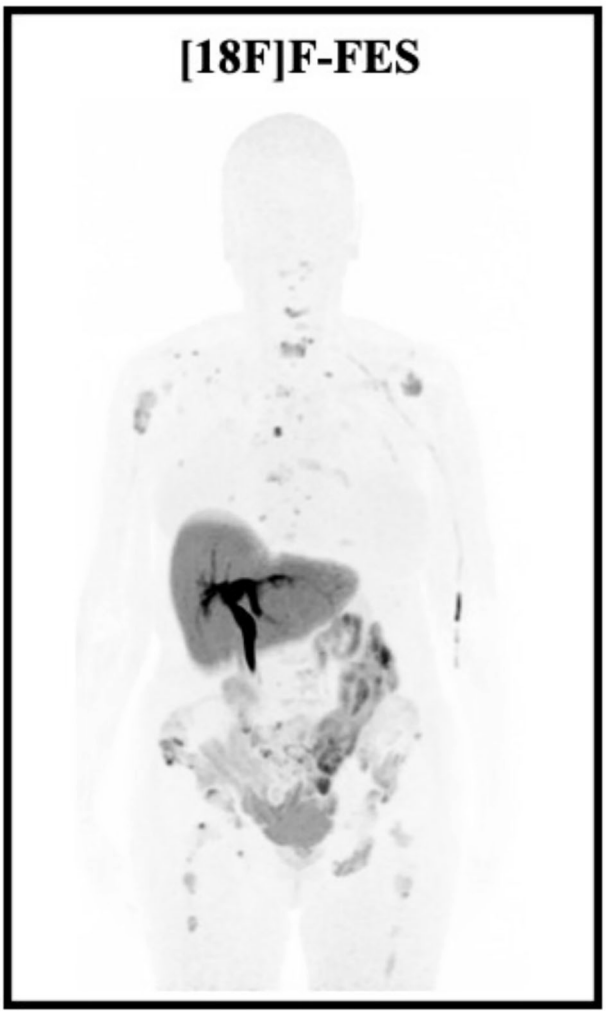

FIGURE 5 | Low intensity MIP images showing the normal biodistribution of [^{18}F]F-FES and multiple bone recurrence metastases of an ILBC, occured 5 years after surgery (SBRII, 15 mm, ER 80%, PR 80%, Ki67 40%, HER2 negative), radiotherapy and hormonotherapy with letrozole.

[^{18}F]F-FES represents one of the clinically most widely used radiopharmaceuticals of this category: a high correlation between [^{18}F]F-FES uptake and estrogen receptor concentration has been demonstrated already in 1980, confirmed on histopathological analysis after tumor excision (98). A recent 2020 meta-analysis by Kurland et al. (99) demonstrated that [^{18}F]F-FES non-invasively characterizes ER ligand binding function in BC lesions with a sensitivity of 0.81 (0.73–0.87) and a specificity of 0.86 (0.68–0.94) compared to the histological standard of reference.

[^{18}F]F-FES PET/CT examinations do not require any specific preparation, however—mainly as a measure of standardization—fasting is recommended and some foods, such as chocolate, should be avoided (100). Nevertheless, some pharmacological aspects have to be taken into account: in case of staging, treatment with ER antagonists (e.g., tamoxifen or fulvestrant) should be discontinued for ≥5 weeks before the examination. Aromatase inhibitors and luteinizing hormone-releasing hormone (LHRH) agonists can be continued (101).

Nowadays, [^{18}F]F-FES PET/CT represents the main non-invasive method for the assessment of ER expression throughout the body, with important therapeutic implications: a low uptake of [^{18}F]F-FES is associated with a higher failure rate of antihormonal treatment (101).

Although current guidelines do not recommend [^{18}F]F-FES PET/CT as a diagnostic tool in patients with ER-positive BC, this radiotracer could be beneficial when conventional and [^{18}F]F-FDG imaging is inconclusive, providing greater specificity than [^{18}F]F-FDG PET/CT. In 2019, Liu et al. (102) investigated whether and how [^{18}F]FES-PET/CT affects the management of 19 newly diagnosed estrogen receptor positive BC patients. A total of 238 lesions was analyzed, there of 216 were detected by [^{18}F]F-FES and 197 by [^{18}F]F-FDG PET/CT, resulting in a sensitivity of 90.8% for [^{18}F]F-FES vs. 82.8% for [^{18}F]F-FDG PET/CT, corroborated by CT and/or other imaging. The application of [^{18}F]F-FES in addition to [^{18}F]F-FDG PET/CT changed the management in 5 of 19 patients (26.3%), highlighting

lesions that were negative or equivocal on [^{18}F]F-FDG. Moreover, [^{18}F]F-FDG PET/CT demonstrates lower sensitivity for ILC, which is almost always (95%) ER-positive. Therefore, Ulaner et al. (103) evaluated 7 metastatic ILC patients with synchronous [^{18}F]F-FDG PET/CT and [^{18}F]F-FES PET/CT. In this cohort, 254 lesions suggestive of malignancy were detected by increased [^{18}F]F-FES uptake (SUVmax, 2.6-17.9), compared to 111 lesions detected by increased [^{18}F]FDG uptake (SUVmax, 3.3-9.9). Notably, [^{18}F]F-FES PET/CT detected more metastatic lesions than [^{18}F]F-FDG PET/CT in 5 of 7 patients (71%). All [^{18}F]F-FDG-positive lesions were also [^{18}F]F-FES-positive. Boers et al. (104) evaluated whether [^{18}F]F-FES PET/CT could resolve the remaining physician's clinical dilemma in 83 BC patients with suspected heterogeneous ER expression. The dilemmas were as follows: inability to determine the extent of metastatic disease or suspected metastatic disease with standard work-up ($n = 52$), unclear ER status of the tumor ($n = 31$), and inability to determine which primary tumor was responsible for the metastases ($n = 17$). A total of 100 PET/CT scans of 83 patients were analyzed: dilemmas were resolved by [^{18}F]F-FES PET/CT in 87 of 100 scans (87%). Furthermore, the frequency of resolved dilemmas was correlated with whether the scans were [^{18}F]FES-positive ($n = 63$) or [^{18}F]F-FES-negative ($n = 37$; $p < 0.001$); demonstrating the usefulness of this radiotracer in cases of clinical dilemma.

In addition, [^{18}F]F-FES PET/CT was found useful in assessing the degree of response to antihormonal therapy in patients with metastatic BC. [^{18}F]F-FES PET/CT can indicate whether the malignant lesions continue to express ER, and thus provide a rationale for continuing or switching lines of antihormonal therapy, or switching to another type of treatment with absent ER expression (105–108). Low or absent uptake of [^{18}F]F-FES in BC lesions correlates with greater resistance to antihormonal therapy, and conversely, patients responding to endocrine therapy showed higher SUV (although no specific SUV thresholds exist to distinguish specific from non-specific uptake) (105, 106, 109). However, a meta-analysis of seven studies (in total 226 patients) by Evangelista et al. (110) showed that the role of [^{18}F]F-FES PET/CT in predicting response to endocrine therapy in advanced BC still remains undetermined: pooled sensitivities and specificities were 63.9% (95% CI: 46.2–79.2%) vs. 66.7% (95% CI: 52.1–79.2%), and 28.6% (95% CI: 17.3–42.2%) vs. 62.1% (95% CI: 48.4–74.5%), for an SUV cutoff of 1.5 and 2.0, respectively.

[^{18}F]F-FES PET/CT has also been used as a tool to predict response to neoadjuvant chemotherapy together with [^{18}F]F-FDG PET/CT in BC patients. In a study of 18 patients, Yang et al. (111) have not found statistically different [^{18}F]F-FDG SUVmax and tumor size among 10 responders and 8 non-responders. In contrast, lower SUVmax [^{18}F]F-FES was found in responders (1.75 ± 0.66 vs. 4.42 ± 1.14; $p = 0.002$) and the [^{18}F]F-FES/[^{18}F]F-FDG SUVmax ratio also showed great value in predicting outcome (0.16 ± 0.06 vs. 0.54 ± 0.22; $p = 0.002$).

The main disadvantages of [^{18}F]F-FES include high uptake in the liver, which may render the assessment of liver metastases difficult; rapid blood clearance, which may lead to lower tumoral uptake; and low selectivity for ERα and ERβ, resulting in reduced specificity of the procedure. In an attempt to overcome these limitations and make PET imaging more specific for ER expression, additional radiopharmaceuticals have been developed, such as 4-fluoro-11β-methoxy-16α-[^{18}F]-fluoroestradiol (4FM-[^{18}F]F-FES) (112) and 1-(2-(2-(2-[^{18}F]fluoroethoxy)ethoxy)ethyl)-1H-1,2,3-triazole-estradiol ([^{18}F]F-FETE) (113).

Progesterone Receptor

Numerous physiologic functions are elicited by the progesterone receptor (PR) through progesterone binding, acting as a ligand-dependent transcription factor (114). The main target tissues are the ovaries, the uterus and mammary gland tissue (115). Progesterone represents a precursor molecule for the synthesis of estrogen, androgen, and adrenocortical steroids (116).

In ∼50% of patients with estrogen-dependent BC, increased progesterone receptor expression is also observed. Therefore, the PR status can provide important prognostic and predictive information. In fact, PR is routinely assessed in clinical practice, since it predicts response to endocrine therapy (114).

In BC, the expression of ERα and PR are closely associated, because functioning ER can increase the expression of PR, which represents a surrogate biomarker for the presence of a functioning estrogenic pathway (117). In fact, ER-/PR+ cases are rare (< 1% of all BCs) (118). In case of ER+/PR+ BC, a response to endocrine treatment will probably be observed (in ∼75%). In contrast, chances of response are lower in ER+/PR- cases (64). However, endocrine therapy still represents an option for these patients, which have an overall poor prognosis owing to their more aggressive disease than PR+ patients (119).

Based on these premises, the main advantage of PET imaging targeting PR is that it serves as a surrogate for ER expression, when this one is saturated by ongoing specific ER therapy.

21-Fluoro-16α-ethyl-19-norprogeserone ([^{18}F]F-FENP) was one of the first [^{18}F]-labeled ligands developed for PET imaging and showed a high affinity for PR, ∼60-fold higher than progesterone, as observed by Pomper et al. (120). However, in clinical PET trials this ligand did not succeed, identifying only 50% of PR+ tumors (121). Owing to its high lipophilicity and metabolism, this radiotracer is characterized by high uptake into liver and adipose tissue, low target-to-background ratio for high background activity, and notable bone uptake for metabolic defluorination (121, 122).

Another radiotracer, [^{18}F]F-FMNP, although characterized by high affinity and specificity for PR, it also showed high lipophilicity and an unfavorable metabolism as [^{18}F]F-FENP, and hence has no clinical application (121).

6α-[^{18}F]-Fluoroprogesterone showed the same limitations, characterized by high absorption in adipose tissue, relatively low target tissue selectivity and high bone absorption due to metabolic defluorination (123).

Among these PR radioligands, the most promising one that was also evaluated clinically is 21-^{18}F-fluoro-16α,17α-[(R)-(1′-α-furylmethylidene)dioxy]-19-norpregn-4-ene-3,20-dione ([^{18}F]F-FFNP), characterized by high PR binding affinity and low non-specific binding (124, 125). Dehdashti et al. demonstrated in their study how [^{18}F]FFNP showed greater

uptake in BC than in healthy breast tissue, and among BCs, greater uptake was observed in PR+ lesions than in PR- lesions (126). Moreover, [^{18}F]F-FFNP is subject to minimal defluorination, resulting in low bone uptake, and it is less affected by hydrogenase metabolism, which unfavorably affects the biodistribution of the above-mentioned other PR radiotracers (121).

Fowler et al. used [^{18}F]F-FFNP to predict response to endocrine therapy in a preclinical model of BC (127). Mammary cell lines (SSM1, SSM2, and SSM3) were implanted into mice and an imaging study was performed to determine whether changes in ERα/PR expression had predictive value for tumor response after endocrine therapy. In another preclinical study, they showed how the uptake of [^{18}F]F-FFNP into the tumor increases after hormonal estrogen therapy, due to synergetic function between estrogen and progesterone receptors; but decreases after the end of therapy in responding lesions, as showed by Linden et al. (64).

In a prospective, phase 2, single-center, single-arm study (NCT02455453) published in 2021, Dehdashti et al. (128) demonstrated for the first time directly in humans the influence of estrogen on tumor progesterone receptors. Forty-three postmenopausal women with advanced ER+ BC underwent two [^{18}F]F-FFNP PET/CT studies on 2 separate days, the second PET being performed after an estradiol challenge (a total dosage of 6 mg of estradiol) administered to detect an eventual "flare reaction" on the second PET. Interestingly, tumoral uptake of [^{18}F]F-FFNP increased only in the 28 subjects with clinical benefit from estrogen therapy (responders), but not in the 15 without clinical benefit (no responders) ($p < 0.0001$), indicating 100% sensitivity and specificity. The authors also showed significantly longer survival ($p < 0.0001$) in responders, which renders this radiotracer highly predictive of response to estrogen therapy in women with ER+ BC, pioneering clinical trials in humans with this radiotracer.

HER2

The use of radiolabeled monoclonal antibodies and derivatives for PET imaging is a field of great scientific interest. As mentioned above, HER2 is a member of the epidermal growth factor receptor (EGFR) family of tyrosine kinases, and is encoded by the HER2 proto-oncogene (9). HER2 is involved in a wide range of cellular processes, such as survival, proliferation, differentiation, maturation, metastatic spread, angiogenesis, invasion, and antiapoptotic functions (129).

HER2/erbB2 oncogene overexpression or amplification occurs in ∼20% of BC patients, representing a negative prognostic factor, as HER2-positive BC is characterized by more aggressive tumor behavior (130, 131). Moreover, HER2 expression may vary between the primary tumor and metastatic lesions (intra-tumor or temporal heterogeneity), with discordant expression rates between 4 and 16% for HER2 expressions, affecting tumor behavior and response to treatment (132). Finally, HER expression may also change during treatment.

For these reasons, it is important to identify a non-invasive tool for monitoring HER2 expression levels *in vivo* during HER2-targeted therapy, particularly for the assessment of treatment response. As mentioned above for hormone receptors, HER2 PET/CT imaging with the development of new probes can also be a useful tool to determine HER2 expression and the location of HER2-positive tumor lesions in a non-invasive and total-body approach (133).

Trastuzumab (Herceptin) is a recombinant G1 immunoglobulin monoclonal antibody, targeting the extracellular domain of HER2, which is widely used in clinical medicine and hence represents an optimal target for the development of a new PET probe (134). [^{89}Zr]Zr-trastuzumab is a PET imaging radiopharmaceutical capable of assessing HER2 expression in BC patients, both in primary and metastatic lesions, qualitatively and quantitatively. It may allow to improve the selection of patients who might benefit most from trastuzumab therapy (135, 136).

The first clinical study with [^{89}Zr]Zr-trastuzumab was performed by Dijkers et al. (136) in 2010 with the aim to evaluate the biodistribution, the optimal dosage and time of radiotracer administration in 14 patients. PET imaging results clearly showed HER2-positive liver, bone, and brain lesions, with a great lesion to background ratio in the liver, spleen, kidneys, and brain. Owing to the long half-life of [^{89}Zr] (78.4 h), imaging could still detect occult metastatic lesions 5 days after [^{89}Zr]Zr-trastuzumab injection. On the other hand, this results in high "radiation exposure." Subsequently, Laforest et al. demonstrated that optimal imaging requires at least 4 days between tracer injection and scanning, even if the liver was the dose-limiting organ for the correct visualization of liver metastasis at 4 days (137).

One of the first human study to evaluate the clinical impact of [^{89}Zr]Zr-trastuzumab PET/CT was conducted by Gebhart et al. (138) in 2016, demonstrating in 56 BC patients that pretreatment imaging of HER2 targeting, combined with early metabolic ([^{18}F]F-FDG) response assessment holds great promise to predict efficacy of HER2-targeting antibody-drug-conjugate trastuzumab emtansine (T-DM1). More recently, Bensch et al. (139) demonstrated that [^{89}Zr]Zr-trastuzumab PET/CT supports clinical decision-making when HER2 status cannot be determined by biopsy.

The shorter half-life of [^{64}Cu] (12.7 h) makes [^{64}Cu]Cu-DOTA-trastuzumab a very attractive radiopharmaceutical for PET imaging. Tamura et al. evaluated PET imaging with [^{64}Cu]Cu-DOTA trastuzumab in six HER2-positive BC patients, showing high activity in blood, but low activity in normal tissue, and a radiation exposure equal to that of [^{18}F]F-FDG PET/CT (140). In addition, this radiopharmaceutical showed good capability to assess HER2 expression *in vivo*, distinguish HER2-positive from HER2-negative BC, and monitor changes in HER2 expression after therapeutic intervention. However, the high liver uptake reduces the ability of this radiotracer for assessing small lesions. This issue can be partially resolved by administering 45 mg of cold trastuzumab before PET to reduce hepatic uptake (141) or by

performing the examination after a standard therapeutic dose of trastuzumab (142).

Another HER2 radiotracer, [^{68}Ga]Ga-DOTA-ABY-002, has only been used for the detection of abdominal BC metastases (143). In 2016, Sorensen et al. (144) tested [^{68}Ga]Ga-DOTA-ABY-025 in 16 patients with metastatic BC in a phase I/II study. Optimal whole-body PET images were obtained at 4 h after injection. Biopsies from 16 metastases in 12 patients were collected for verification of HER2 expression by immunohistochemistry and *in-situ* hybridization. PET SUV correlated with biopsy-derived HER2 scores ($r = 0.91$, $p < 0.001$) and uptake was five times higher in HER2-positive than in HER2-negative lesions with no overlap ($p = 0.005$). With regard to the dosimetry, the highest absorbed organ doses were seen in the kidneys, followed by the liver (145).

In order to overcome the problem of high background uptake and potential issues related to cross-calibration of scanning devices, Sandberg et al. (146) aimed to investigate the utility of a tumor-to-reference tissue-ratio (T/R) as a HER2 status discrimination strategy in 16 patients with HER2-positive/negative metastasized BC, scanned with [^{68}Ga]Ga-ABY-025 PET/CT. Spleen was the best reference tissue and spleen-T/R was highly correlated to PET SUV in metastases after 2 h ($r = 0.96$, $p < 0.001$), reaching an accuracy of 100% for discriminating immunohistochemistry (IHC) HER2-positive and negative metastases at 4 h (PET) after injection.

Overall, clinical data on HER2 imaging in PET are still few and limited, but own great potential, particularly with encouraging preclinical data on the horizon.

INTEGRINS TARGETED RADIOTRACERS

The integrins are a family of transmembrane proteins involved in many fundamental cellular processes, such as interaction between the cell and the extracellular matrix, and mediation between cells. Moreover, the integrins influence extracellular and intracellular signaling pathways, including apoptosis, and play also a key role in tumor progression and metastasis (147). In particular, the αvβ3 subclass is involved in tumor transformation, angiogenesis, local invasiveness, and metastatic potential. It is known to be over-expressed by both angiogenic endothelium and cells in several tumor types, including BC (148). The αvβ3 subclass is involved among various angiogenic signaling cascades, such as the vascular endothelial growth factor (VEGF) pathway. The inhibition of VEGF significantly suppresses the expression of αvβ3 on tumor cells, with reduced microvascular density, thus it has been proposed as a marker of angiogenic activity (149). Bevacizumab (anti-VEGF antibody) represents one of the most widely used drugs for anti-angiogenic treatment, through inhibition of the VEGF pathway, in several tumor types, such as in non-small cell lung cancer, colorectal cancer, and glioma (150). Arginine-glycine-aspartic acid (RGD) peptide ligands have shown high affinity for αvβ3-integrin and can be radiolabeled for PET imaging of angiogenesis or tumor development (151, 152). In a preclinical study performed in mice with BC, scans were performed at baseline and after bevacizumab therapy. [^{68}Ga]Ga-TRAP (RGD)3 uptake was reduced in mice treated with the VEGF antibody compared to the untreated group, where uptake did not change significantly (153). With the ability to non-invasively visualize αvβ3 expression by PET in BC patients, important data on the integrin levels in tumor lesions might be obtained with the goal select the most suitable patients for antiangiogenic treatment and to assess the degree of response to this type of therapy. In fact, in a clinical study of 16 patients with BC (154), it was observed that [^{18}F]F-Galacto-RGD was absorbed by all tumor lesions, both primary and metastatic ones, although with heterogeneous uptake levels. [^{68}Ga]Ga-NODAGA-THERANOST, a second-generation compound, was used in 2 patients, one of them with BC, showing promising data (155). [^{18}F]F-fluciclatide ([^{18}F]F-AH111585) appears to be more stable, safe, and well-tolerated (156, 157) providing a good target/background ratio. This probe allows detection of both primary and metastatic BC lesions, although evaluation of liver metastases may be suboptimal due to high physiological hepatic uptake (66). Even with [^{18}F]F-fluciclatide, tumor uptake was observed to vary considerably between individuals and between tumor types, and even between tumors of the same type within a patient. In order to assess this heterogeneity, Tomasi et al. (158) employed a dynamic acquisition of [^{18}F]F-fluciclatide PET data in BC patients with metastases. In 8 patients with BC [^{18}F]F-FPPRGD2 was used to evaluate the expression of integrin avβ3. This probe is characterized by high specificity, although showing high uptake in the liver and kidneys, which may limit the evaluation of metastases in these organs (159). Gaykema et al. studied [^{89}Zr]Zr-bevacizumab in 23 patients with BC undergoing PET imaging 4 days after administration, which is considered the optimal time-point and it is possible thanks to the long half-life of [^{89}Zr] (78.4 h). They observed a significantly higher uptake in tumor lesions than in healthy tissue, and that luminal B tumors showed greater uptake compared to luminal A tumors. However, this radiotracer overall yielded low sensitivity in detecting lymph node lesions (160).

CHOLINE ANALOGS RADIOTRACERS

Since many years, it has been observed—mainly through spectroscopy MRI studies—that in many tumor types there is an altered choline metabolism (161). Choline is an essential component of the cell membrane and a building block for the synthesis of fatty acids (162). When choline enters the cell, it is phosphorylated by choline kinase-α, turning into phosphocholine, which is trapped inside the cell. This phenomenon has been observed to increase with parathyroid adenoma mainly in primary hyperparathyroidism (163) and with malignant transformation in some tumor types, such as BC (particularly HER2 BC) (164). Although most clinical trials have been performed for prostate cancer (165), promising results have also been obtained with N-[^{11}C]methyl-choline ([^{11}C]C-choline) in BC patients. Increased uptake in BC compared to normal tissue was observed, which was related to the expression and activity of choline kinase-α since choline is required for membrane synthesis in actively proliferating cells

(166). After several case reports, in 2009, Contractor et al. (167) first evaluated the use of [^{11}C]C-choline PET/CT in in 32 individuals with primary or metastatic ER–positive BC. Their study demonstrated that breast tumors were well-visualized in 30 of 32 patients with good tumor background ratio. In 2010, Kenny et al. (168) demonstrated the reproducibility of the [^{11}C]C-choline PET/CT uptake variables in 21 BC patients, performing a dual time point evaluation. They also demonstrated that trastuzumab therapy decreases [^{11}C]C-choline uptake in BC lesions. One of the main disadvantages of this PET imaging method is the high physiological hepatic uptake, which may limit the evaluation of liver metastases. Only a few clinical studies have been performed on [^{18}F]F-choline in BC patients, limited to case reports (169). More recently, Saad et al. (170) described the pathological distribution of [^{18}F]F-choline PET/CT scan, acquired 40 min after injection, and pitfalls in 21 BC patients. All patients showed potentially false negative lesions, predominantly caused by physiological uptake in the liver, spleen, pancreas, bowel, axial skeleton (85–100%), inflammation and benign lesions (4.7%), and appendicular skeleton (4.7–19.0%). Also, [^{18}F]F-choline uptake was higher in lesions of premenopausal women.

PROSTATE-SPECIFIC MEMBRANE ANTIGEN RADIOTRACERS

Prostate-specific membrane antigen (PSMA) is a type II transmembrane protein strongly overexpressed in most prostate cancer (PCa) cells, although also normally expressed in benign prostate tissue at lower levels (171, 172). In addition to prostate cancer, several studies have demonstrated increased PSMA expression in other malignancies, such as lung cancer, colorectal cancer, renal cell carcinoma, and BC (173, 174). Several case reports have shown avid PSMA uptake by both incidentally detected male breast cancer primary and metastases (175–184), but also false-positive uptake associated with gynecomastia. In 2017, Sathekge et al. (185) reported on imaging findings using [^{68}Ga]PSMA-HBED-CC ([^{68}Ga]Ga-PSMA-11) PET/CT in a series of 19 breast carcinoma female patients (9 treatment-naive patients, 5 patients with loco-regional recurrence and 5 patients before chemotherapy). Out of 81 tumor lesions identified with routinely performed staging examinations (including [^{18}F]F-FDG PET/CT in 6/19 patients), 84% were identified on [^{68}Ga]Ga-PSMA-11 PET/CT. No significant difference was found between [^{68}Ga]Ga-PSMA-11 and [^{18}F]F-FDG detection of lesions. No significant difference in PSMA uptake was found between progesterone receptor-positive and progesterone receptor-negative lesions. However, authors documented the absence of PSMA expression in normal vascular endothelium, as well as its limited expression on the luminal side of the intestinal epithelium. These results, although preliminary, appear promising for a possible future use of PSMA not only in a diagnostic but also in a theragnostic setting (radioligand therapy) in BC patients. In 2018, Tolkach et al. (182) reported the results of a compassionate treatment with [^{177}Lu]Lu-PSMA performed in a 38-year-old woman with TNBC due to rapid progress after a wide range of systemic therapies. The [^{177}Lu]Lu-PSMA treatment was approved after PSMA receptor status was demonstrated in [^{68}Ga]Ga-PSMA-11 PET/CT. The patient obtained 7.5 GBq [^{177}Lu]Lu-PSMA twice with a 4-week interval. The patient unfortunately progressed under therapy, but the low toxicity suggests further studies to elucidate the efficacy of PSMA-directed therapy, especially in cases of TNBC.

MOLECULAR IMAGING OF IMMUNOTHERAPY (IMMUNOPET)

Among the new therapeutic strategies for metastatic BC, immunotherapy has been gaining tremendous importance in recent years. Although more established in the treatment of other cancers, such as lung cancer (186) and melanoma, immunotherapy with immune-checkpoint inhibitors (ICIs) has recently acquired a predominant role in TNBC, which tends to be characterized by increased expression of programmed cell death protein 1 (PD-1), programmed cell death ligand 1 (PD-L1), a higher prevalence of tumor-infiltrating lymphocytes (TILs) and a higher mutational burden (187).

The Food and Drugs Administration (FDA) has approved combined chemotherapy and immunotherapy treatment with both anti PD-L1 (such as atezolizumab) and anti PD-1 (such as pembrolizumab) monoclonal antibodies for PD-L1+ TNBC (188). New indications for the use of these combination therapies are also expanding to other patient populations, such as advanced hormone receptor-positive (HR+) BC or HER-2 positive patients who are refractory to standard therapy (187).

Although the response to immunotherapy is very heterogeneous, patients who have achieved a response have a prolonged overall survival. Therefore, the main challenge is to develop and identify new biomarkers predictive of benefit from and resistance to immunotherapy. [^{18}F]F-FDG is not able to assess the finer mechanisms underlying tumoral IC expression and resistance to immunotherapy. For this reason, new molecular imaging probes have been developed to improve our knowledge on the tumor microenvironment (TME), immune system and ICIs (189). New PET radiotracers targeting IC proteins may allow to systematically map PD-L1 tumor expression and/or PD-1 and cytotoxic T-lymphocyte associated protein 4 (CTLA-4) cell expression, in both spatial (whole-body) and temporal dimension, potentially providing added value for therapy and patient selection (186, 189).

In 2019, the first-in-human study by Bensch at al. (190) evaluated [^{89}Zr]Zr-atezolizumab PET/CT performance in 22 patients with metastatic bladder cancer, non-small cell lung cancer (NSCLC), or TNBC. [^{89}Zr]Zr-atezolizumab uptake was found to be physiologically high in bone marrow, intestine, kidneys, and liver, but low in brain, subcutaneous tissue, muscle, compact bone, and lung, while the uptake in lymph nodes and spleen depended on the activation state of the immune system. They found that pre-treatment radiotracer uptake better correlated with PFS and OS, compared to conventional IHC staining of PD-L1, highlighting the limitations of a single biopsy

evaluation. Tumoral [^{89}Zr]Zr-atezolizumab uptake was generally high (mean SUVmax of 10.4), but often with high intra-tumoral, inter-tumoral and inter-patient heterogeneity. Despite several new probes studied in the preclinical field, to date no other probes have been evaluated in humans with BC.

PET radiotracers with a labeled monoclonal antibody targeting the inducible T-cell costimulator (ICOS) could also gain an importance in this field, distinguishing tumor progression from pseudo-progression and identifying potential non-responding patients (patients which ICOS PET showing low or no uptake of activated T cells) and/or lesions. However, these radiotracers have yet not been studied in humans with BC (189).

Although immuno-PET radiotracers are still not entered clinical practice, in the future they may help clinicians to select patients who are good candidates for immunotherapy, identifying response earlier and potentially distinguish tumor progression from pseudo-progression.

FIBROBLAST ACTIVATION PROTEIN-α TARGETED RADIOTRACERS

As previously mentioned, the TME is a complex system of transformed tumor cells and other cellular and molecular components that regulate tumor development (189). In this context, cancer-associated fibroblasts (CAF) play an essential role in tumor growth, TME function, metastatic spread, and therapy resistance through potent immunosuppressive activity, conferring resistance to immune-based therapies (191).

In the last decade, researchers have attempted to better study CAF cells and their role in cancer evolution, which is correlated with T-cell immunosuppression and lead to poor clinical outcome (192), also by developing specific probes, such as new radiotracers targeting CAF-dependent pathways.

Fibroblast activation protein-α (FAPα), a transmembrane serine protease and marker of CAF activation, is overexpressed on CAF cell membrane and stroma in ∼90% of epithelial neoplasms, whereas it is vastly absent in normal stromal cells (193). In 2018, researchers at the University of Heidelberg have introduced PET imaging of FAP expression in cancer, producing a [^{68}Ga]-labeled FAP inhibitor (FAPi), derived from quinoline peptidomimetics, that binds with high affinity to FAP expressed on CAFs (194, 195). This new radiotracer seems extremely promising due to the excellent visualization of various kinds of tumors, owing to the high tumor-to-background ratio (TBR) (196, 197).

In 2021, two different studies (198, 199) compared [^{68}Ga]Ga-FAPi PET/CT and [^{18}F]F-FDG PET/CT in patients with BC. Elboga et al. (198) aimed to detect additional lesions in BC patients that may affect further chemotherapy options in 48 patients. The study demonstrated more lesions in all categorized regions in [^{68}Ga]Ga-FAPi PET/CT with higher uptake compared to [^{18}F]F-FDG PET/CT. In treatment response assessment of the post-chemotherapy group, [^{68}Ga]Ga-FAPi PET/CT shifted 12 cases (12/24) from stable disease (SD) to progressive disease (PD) compared to [^{18}F]F-FDG PET/CT, because of the assessment of lesions that were occult on [^{18}F]F-FDG PET/CT. Kömek et al. (199) evaluated the assessment of primary tumor and metastases in 20 patients with histopathologically confirmed primary and recurrent BC. [^{68}Ga]Ga-FAPi PET/CT was superior to [^{18}F]F-FDG PET/CT in detecting breast lesions, as well as liver, bone, lymph node and brain metastases in terms of patient-based and lesion-based assessment, with higher uptake values compared to [^{18}F]F-FDG PET/CT. The sensitivity and specificity of [^{68}Ga]Ga-FAPi in detecting primary breast lesions were 100 and 95.6%, respectively, while [^{18}F]F-FDG yielded 78.2 and 100%, respectively.

FAPi may also serve as theragnostic probes: the high TBR can be exploited by labeling FAPi with alpha- or beta-emitting isotopes to generate a potentially new intriguing radioligand therapy for BC, among other cancers (200–203).

GASTRIN-RELEASING PEPTIDE RECEPTOR TARGETED RADIOTRACERS

Gastrin releasing peptide receptor (GRPR) belongs to subtype II of the bombesin receptor (BBN) family. It is a seven-transmembrane G protein-coupled receptor conjugated with BBN (204). The main physiological role of gastrin-releasing peptide (GRP) is the release of gastrin, contributing to the regulation of enteric function, but it may also hold a function in carcinogenesis and cell proliferation (205). Different studies have demonstrated GRPR overexpression in several cancer types, such as lung, gastric, pancreatic, prostate, colorectal, ovarian and endometrial cancer, and in glioma (206–208). Overexpression of GRPR has also been observed in BC, both in invasive ductal carcinoma (65%) and invasive lobular carcinoma (68%) (209).

Different molecular probes for visualizing GRPR expression have been developed (210, 211) and were subsequently used in preclinical and clinical studies. Notably, both agonists for GRPR and antagonists for GRPR have been developed. Particularly the antagonists have demonstrated improved image contrast and uptake compare to agonists, without adverse gastrointestinal effects (212).

Stoykow et al. (213) used [^{68}Ga]Ga-RM2 PET/CT (RM2 is a GRPR antagonist) in patients referred for staging BC: an upstaging was found in 7/15 patients (47%) due to the detection of suspicious lymph nodes, owing to a favorable TBR. All PET-positive primary tumors were ER+ and PR+ (13/13) in contrast to only 1/5 PET-negative tumors, demonstrating that [^{68}Ga]Ga-RM2 uptake correlates with ER expression in primary tumors of untreated patients.

More recently, Michalski et al. (214) assessed tumor binding of RM2 before and after neoadjuvant chemotherapy (NAC) in 7 primary BC, demonstrating a significantly reduced [^{68}Ga]Ga-RM2 uptake on post-NAC PET/CT in all primary tumors. Moreover, the residual [^{68}Ga]Ga-RM2 uptake in ER-positive primary BC correlated well with residual vital tumor size after NAC.

In 2021, a new study from the same group (215) on eight female patients with initial ER+ BC, demonstrated how [^{68}Ga]Ga-RM2 PET/CT could support treatment decisions in

these patients, guide radiotherapy planning in oligometastatic patients or select patients for RM2 radioligand therapy.

OTHER NEW RADIOTRACERS FOR MOLECULAR IMAGING IN BREAST CANCER

Several other radiotracers have been studied for BC assessment.

Neuroendocrine differentiation is observed in up to 20% of BC (216). BCs with neuroendocrine differentiation (NE BCs) are characterized by an overexpression of somatostatin receptors (SSTRs), as well as synaptophysin and chromogranin positivity (217). NE BCs may benefit from a non-invasive, whole-body PET/CT evaluation using SSTR radiotracers (218, 219) and in selected cases could also benefit from a theragnostic approach with peptide receptor radionuclide therapy (PRRT) (220, 221).

The study of proteins responsible for drug resistance has attracted the interest of many researchers in recent years, especially the study of P-glycoprotein (Pgp) (also known as multidrug-resistance protein 1 and ABCB1), which is a membrane protein able to actively remove drugs from the cell, with important implications in drug resistance in oncology (222). Studies of PET radiotracers, labeled with [^{11}C] or [^{18}F] and directed against Pgp are still in a preclinical phase. Nevertheless, tracers have been developed for both Pgp substrates and Pgp inhibitors (223). To date, only one feasibility study (dosimetric evaluation and tracer biodistribution assessment) was performed in 2011 by Kurdziel et al. (224), who administered [^{18}F]-fluoropaclitaxel to 3 healthy volunteers and 3 patients with untreated BC (neoadjuvant chemotherapy candidates, tumor size $>$ 2 cm), demonstrating the possible use of this radiotracer as a surrogate for paclitaxel.

Another biomarker of great interest in the field of molecular imaging is the imaging of apoptosis, which could help to drive therapeutic decisions, especially in the field of radiotherapy (225). The most studied tracers in this area target:

(1) annexin V, which detects phosphatidylserine expression on the cell surface. However, annexin V radiotracers have not performed well, mainly due to high background owing to slow blood clearance (226, 227);

(2) 2-(5-fluoro-pentyl)-2-methyl-malonic acid (ML-10), a lower molecular weight probe, labeled with [^{18}F] (228);

(3) caspases, cysteine-aspartate-specific proteases, activated by intrinsic and extrinsic apoptotic pathways. A common treatment strategy is the induction of apoptosis in tumors, *via* the activation of the caspase cascade. Particular efforts have been made in the study of caspase 3-related radiotracers (229), such as [^{18}F]F-ICMT-11, which has already provided promising results in BC patients (230).

Another field of growing interest is acetate radiotracers. Under metabolic stress, acetate becomes the main metabolic substrate for cancer cells instead of glucose. Acetate provides lipids and fatty acids and is particularly used by BC cells, which internalize it. Afterwards, acetate therefore binds to Co-A by acetyl-CoA synthetase (ACSS, EC 6.2.1.1), forming acetyl-CoA. It is precisely ACSS and its inhibitors that have been used to create radiotracers for acetate metabolism (231–233).

DISCUSSION

Breast cancer research is focusing on developing new drugs, that work only in tumors with a certain biomarker or mutation (2, 8). This has paved the way for improved survival of BC patients, assuming better individualization of the correct therapy for each tumor in each patient (personalized therapy) and assuming a prompt shift in therapy as the molecular and behavioral characteristics of the tumor change (temporal heterogeneity). In this scenario, PET imaging of ER and PR expression receptors is an attractive solution to the caveat of pathologic assessment by IHC and has an essential role in identifying patients who are candidates for hormone therapy and determining response to treatment. In addition, acquired resistance is a hallmark of endocrine therapy, and PET could be used to optimize clinical decision-making when resistance is acquired (234). Similarly, PET imaging of HER2 can provide important non-invasive, whole-body information about the tumor expression of this receptor. Indeed, as mentioned above, the development of HER2-specific therapies (such as trastuzumab) has resulted in improved outcomes in patients with HER2-positive tumors considered to have a poor prognosis (12). Moreover, dual PET imaging of ER and PR receptors' ligands combined with metabolic imaging ([^{18}F]F-FDG), or better imaging of aggressive tumors (such as HER2 imaging or PSMA imaging) could improve assessment of tumor aggressiveness, allowing easier identification of targeted therapy for each patient.

These new radiopharmaceuticals may also provide an additional patient assessment tool for de-escalation, which is currently gaining interest in breast cancer not only in the surgical setting but also in terms of discontinuation of systemic therapy and reduction/interruption of radiotherapy treatment (8). In the balance between an acceptable increase in the risk of relapse and a potential decrease in side effects, radiopharmaceuticals such as FAPi, PSMA, and ligands of the ER, PR, and HER2 receptors can support the choice of de-escalation, providing additional information on the assessment of response compared with [^{18}F]F-FDG, both in case of false-negative [^{18}F]F-FDG PET (related to FDG-avidity of tumor type) and false-positive [^{18}F]F-FDG PET (related to post-therapy changes, especially after radiotherapy).

Finally, the development of these new radiopharmaceuticals has introduced the theragnostics concept into the BC field, increasing the possibility of more personalized treatments based on individual and tumor characteristics soon (235–238).

CONCLUSION

In recent decades, the advancement of modern medicine through multidisciplinary and translational approaches has contributed to a better understanding of the mechanisms and molecules involved in the development of breast cancer and responsible for its genotypic and phenotypic heterogeneity.

In nuclear medicine, these discoveries have allowed the development of new diagnostic biomarkers capable of assessing *in-vivo* and non-invasively several key features of breast cancer that are relevant for diagnosis, staging and restaging. These new probes can support clinical decision-making and patient selection by evaluating specific therapeutic targets for an improved assessment of response to specific treatments.

Molecular imaging is becoming an indispensable tool to support collaboration among health professionals involved in the fight against BC in order to achieve a more personalized therapy, through an increasingly accurate characterization of lesions using probes that can refine the ability to predict prognosis and response to therapy.

It is expected that these probes will be usable in the future also for therapeutic purposes owing to an increasingly prudent use of therapeutic radionuclides and the development of radioligand therapy.

DATA AVAILABILITY STATEMENT

The original contributions presented in the study are included in the article/supplementary material, further inquiries can be directed to the corresponding author.

AUTHOR CONTRIBUTIONS

MiB, VL, and DD: substantial contributions to the conception or design of the work. MiB, VL, MR, and RL: literature search and article selection. MiB and VL: drafting of the manuscript. MR, RL, MaB, AmB, DN, SP, AnB, GA, NQ, RA, SM, CD'A, ET, MH, AP, and DD: critical revision of the manuscript for important intellectual content. MiB, VL, RA, SM, CD'A, ET, MH, AP, and DD: supervision. All authors have read and agreed to the published version of the manuscript. All authors contributed to the article and approved the submitted version.

FUNDING

MH is a recipient of grants from GE Healthcare, grants for translational and clinical cardiac and oncological research from the Alfred and Annemarie von Sick Grant legacy, and grants from the Artificial Intelligence in oncological Imaging Network by the University of Zurich.

ACKNOWLEDGMENTS

Figures 1, **2** have been created with BioRender.com.

REFERENCES

1. Sung H, Ferlay J, Siegel RL, Laversanne M, Soerjomataram I, Jemal A, et al. Global cancer statistics 2020: GLOBOCAN estimates of incidence and mortality worldwide for 36 cancers in 185 countries. *CA Cancer J Clin.* (2021) 71:209–49. doi: 10.3322/caac.21660
2. Harbeck N, Penault-Llorca F, Cortes J, Gnant M, Houssami N, Poortmans P, et al. Breast cancer. *Nat Rev Dis Prim.* (2019) 5:1–31. doi: 10.1038/s41572-019-0111-2
3. Cardoso F, Kyriakides S, Ohno S, Penault-Llorca F, Poortmans P, Rubio IT, et al. Early breast cancer: ESMO Clinical Practice Guidelines for diagnosis, treatment and follow-up. *Ann Oncol.* (2019) 30:1194–220. doi: 10.1093/annonc/mdz173
4. Gennari A, André F, Barrios CH, Cortés J, de Azambuja E, DeMichele A, et al. ESMO Clinical Practice Guideline for the diagnosis, staging and treatment of patients with metastatic breast cancer. *Ann Oncol.* (2021) 32:1475–95. doi: 10.1016/j.annonc.2021.09.019
5. Salaün PY, Abgral R, Malard O, Querellou-Lefranc S, Quere G, Wartski M, et al. Good clinical practice recommendations for the use of PET/CT in oncology. *Eur J Nucl Med Mol Imaging.* (2020) 47:28–50. doi: 10.1007/s00259-019-04553-8
6. Kikano EG, Avril S, Marshall H, Jones RS, Montero AJ, Avril N. PET/CT variants and pitfalls in breast cancers. *Semin Nucl Med.* (2021) 51:474–84. doi: 10.1053/j.semnuclmed.2021.04.005
7. Erber R, Hartmann A. Histology of luminal breast cancer. *Breast Care.* (2020) 15:327–36. doi: 10.1159/000509025
8. Loibl S, Poortmans P, Morrow M, Denkert C, Curigliano G. Breast cancer. *Lancet.* (2021) 397:1750–69. doi: 10.1016/S0140-6736(20)32381-3
9. Hamilton E, Shastry M, Shiller SM, Ren R. Targeting HER2 heterogeneity in breast cancer. *Cancer Treat Rev.* (2021) 100:102286. doi: 10.1016/j.ctrv.2021.102286
10. Perou CM, Sørile T, Eisen MB, Van De Rijn M, Jeffrey SS, Ress CA, et al. Molecular portraits of human breast tumours. *Nature.* (2000) 406:747–52. doi: 10.1038/35021093
11. Burguin A, Diorio C, Durocher F. Breast cancer treatments: updates and new challenges. *J Pers Med.* (2021) 11:808. doi: 10.3390/jpm11080808
12. Loibl S, Gianni L. HER2-positive breast cancer. *Lancet.* (2017) 389:2415–29. doi: 10.1016/S0140-6736(16)32417-5
13. Cserni G, Quinn CM, Foschini MP, Bianchi S, Callagy G, Chmielik E, et al. Triple-negative breast cancer histological subtypes with a favourable prognosis. *Cancers.* (2021) 13:5694. doi: 10.3390/cancers13225694
14. Cruz-Tapias P, Rubiano W, Rondón-Lagos M, Villegas VE, Rangel N. Intrinsic subtypes and androgen receptor gene expression in primary breast cancer. A meta-analysis. *Biology.* (2021) 10:834. doi: 10.3390/biology10090834
15. Liberati A, Altman DG, Tetzlaff J, Mulrow C, Gøtzsche PC, Ioannidis JPA, et al. The PRISMA statement for reporting systematic reviews and meta-analyses of studies that evaluate healthcare interventions: explanation and elaboration. *BMJ.* (2009) 339:b2700. doi: 10.1136/bmj.b2700
16. Peñuelas I, Domínguez-Prado I, García-Velloso MJ, Martí-Climent JM, Rodríguez-Fraile M, Caicedo C, et al. PET tracers for clinical imaging of breast cancer. *J Oncol.* (2012) 2012:9. doi: 10.1155/2012/710561
17. Han S, Choi JY. Impact of 18F-FDG PET, PET/CT, and PET/MRI on staging and management as an initial staging modality in breast cancer: a systematic review and meta-analysis. *Clin Nucl Med.* (2021) 46:271–282. doi: 10.1097/RLU.0000000000003502
18. Ulaner GA. PET/CT for patients with breast cancer: where is the clinical impact? *Am J Roentgenol.* (2019) 213:254–65. doi: 10.2214/AJR.19.21177
19. Buck A, Schirrmeister H, Kühn T, Shen C, Kalker T, Kotzerke J, et al. FDG uptake in breast cancer: correlation with biological and clinical prognostic parameters. *Eur J Nucl Med.* (2002) 29:1317–23. doi: 10.1007/s00259-002-0880-8
20. Koo HR, Park JS, Kang KW, Cho N, Chang JM, Bae MS, et al. 18F-FDG uptake in breast cancer correlates with immunohistochemically defined subtypes. *Eur Radiol.* (2014) 24:610–8. doi: 10.1007/s00330-013-3037-1
21. Kitajima K, Fukushima K, Miyoshi Y, Nishimukai A, Hirota S, Igarashi Y, et al. Association between 18F-FDG uptake and molecular subtype of breast cancer. *Eur J Nucl Med Mol Imaging.* (2015) 42:1371–7. doi: 10.1007/s00259-015-3070-1
22. Boers J, de Vries EFJ, Glaudemans AWJM, Hospers GAP, Schröder CP. Application of PET tracers in molecular imaging for breast cancer. *Curr Oncol Rep.* (2020) 22:1–16. doi: 10.1007/S11912-020-00940-9

23. Kitajima K, Miyoshi Y. Present and future role of FDG-PET/CT imaging in the management of breast cancer. *Jpn J Radiol.* (2016) 34:167–80. doi: 10.1007/s11604-015-0516-0
24. Bertagna F, Treglia G, Orlando E, Dognini L, Giovanella L, Sadeghi R, et al. Prevalence and clinical significance of incidental F18-FDG breast uptake: a systematic review and meta-analysis. *Jpn J Radiol.* (2014) 32:59–68. doi: 10.1007/s11604-013-0270-0
25. Dawood S, Merajver SD, Viens P, Vermeulen PB, Swain SM, Buchholz TA, et al. International expert panel on inflammatory breast cancer: consensus statement for standardized diagnosis and treatment. *Ann Oncol.* (2011) 22:515–23. doi: 10.1093/annonc/mdq345
26. Metser U, Even-Sapir E. Increased 18F-Fluorodeoxyglucose uptake in benign, nonphysiologic lesions found on whole-body positron emission tomography/computed tomography (PET/CT): accumulated data from four years of experience with PET/CT. *Semin Nucl Med.* (2007) 37:206–22. doi: 10.1053/j.semnuclmed.2007.01.001
27. Tania Rahman W, Neal CH, Nees AV, Brown RKJ. Management of incidental breast lesions detected at nuclear medicine examinations. *Radiol Imaging Cancer.* (2020) 2:e190037. doi: 10.1148/rycan.2020190037
28. Dong A, Wang Y, Lu J, Zuo C. Spectrum of the breast lesions with increased 18F-FDG uptake on PET/CT. *Clin Nucl Med.* (2016) 41:543–57. doi: 10.1097/RLU.0000000000001203
29. Kim HO, Kim BS, Kang SY, Bang JI, An J, Kim JH, et al. Metabolic changes in breast cancer on dual-time-point 18F-FDG PET/CT imaging according to primary tumor uptake and background parenchymal enhancement. *Ann Nucl Med.* (2020) 34:942–51. doi: 10.1007/s12149-020-01525-z
30. Yamagishi Y, Koiwai T, Yamasaki T, Einama T, Fukumura M, Hiratsuka M, et al. Dual time point 18F-fluorodeoxyglucose positron emission tomography/computed tomography fusion imaging (18F-FDG PET/CT) in primary breast cancer. *BMC Cancer.* (2019) 19:1–12. doi: 10.1186/s12885-019-6315-8
31. Haukaas TH, Euceda LR, Giskeødegård GF, Bathen TF. Metabolic portraits of breast cancer by HR MAS MR spectroscopy of intact tissue samples. *Metabolites.* (2017) 7:18. doi: 10.3390/metabo7020018
32. Leskinen-Kallio S, Joensuu H, Ruotsalainen U, Nagren K, Lehikoinen P. Uptake of 11C-methionine in breast cancer studied by PET.An association with the size of S-phase fraction. *Br J Cancer.* (1991) 64:1121–4. doi: 10.1038/bjc.1991.475
33. Huovinen R, Leskinen-Kallio S, Någren K, Lehikoinen P, Ruotsalainen U, Teräs M. Carbon-11-methionine and pet in evaluation of treatment response of breast cancer. *Br J Cancer.* (1993) 67:787–91. doi: 10.1038/bjc.1993.143
34. Ulaner GA, Schuster DM. Amino acid metabolism as a target for breast cancer imaging. *PET Clin.* (2018) 13:437–44. doi: 10.1016/j.cpet.2018.02.009
35. Lindholm P, Lapela M, Någren K, Lehikoinen P, Minn H, Jyrkkiö S. Preliminary study of carbon-11 methionine PET in the evaluation of early response to therapy in advanced breast cancer. *Nucl Med Commun.* (2009) 30:30–6. doi: 10.1097/MNM.0b013e328313b7bc
36. Jansson T, Westlin JE, Ahlström H, Lilja A, Långström B, Bergh J. Positron emission tomography studies in patients with locally advanced and/or metastatic breast cancer: a method for early therapy evaluation? *J Clin Oncol.* (1995) 13:1470–7. doi: 10.1200/JCO.1995.13.6.1470
37. Inoue T, Kim EE, Wong FCL, Yang DJ, Bassa P, Wong WH, et al. Comparison of fluorine-18-fluorodeoxyglucose and carbon-11-methionine PET in detection of malignant tumors. *J Nucl Med.* (1996) 37:1472–6.
38. Lizarraga KJ, Allen-Auerbach M, Czernin J, DeSalles AAF, Yong WH, Phelps ME, et al. (18)F-FDOPA PET for differentiating recurrent or progressive brain metastatic tumors from late or delayed radiation injury after radiation treatment. *J Nucl Med.* (2014) 55:30–6. doi: 10.2967/JNUMED.113.121418
39. Zhang-Yin JT, Girard A, Bertaux M. What does pet imaging bring to neuro-oncology in 2022? A review. *Cancers.* (2022) 14:879. doi: 10.3390/CANCERS14040879
40. Bauckneht M, Capitanio S, Raffa S, Roccatagliata L, Pardini M, Lapucci C, et al. Molecular imaging of multiple sclerosis: from the clinical demand to novel radiotracers. *EJNMMI radiopharm chem.* (2019) 4:6. doi: 10.1186/s41181-019-0058-3
41. Harris SM, Davis JC, Snyder SE, Butch ER, Vavere AL, Kocak M, et al. Evaluation of the biodistribution of 11C-methionine in children and young adults. *J Nucl Med.* (2013) 54:1902–8. doi: 10.2967/jnumed.112.118125
42. Marcus C, Abiodun-Ojo OA, Jani AB, Schuster DM. Clinical utility of (18)F-Fluciclovine PET/CT in recurrent prostate cancer with very low (≤0.3 ng/mL) prostate-specific antigen levels. *Am J Nucl Med Mol Imaging.* (2021) 11:406–14.
43. Laudicella R, Albano D, Alongi P, Argiroffi G, Bauckneht M, Baldari S, et al. 18F-FACBC in prostate cancer: a systematic review and meta-analysis. *Cancers.* (2019) 11:1348. doi: 10.3390/cancers11091348
44. Biscontini G, Romagnolo C, Cottignoli C, Palucci A, Fringuelli FM, Caldarella C, et al. 18f-fluciclovine positron emission tomography in prostate cancer: a systematic review and diagnostic meta-analysis. *Diagnostics.* (2021) 11:304. doi: 10.3390/diagnostics11020304
45. Ulaner GA, Goldman DA, Gönen M, Pham H, Castillo R, Lyashchenko SK, et al. Initial results of a prospective clinical trial of 18FFluciclovine PET/CT in newly diagnosed invasive ductal and invasive lobular breast cancers. *J Nucl Med.* (2016) 57:1350–6. doi: 10.2967/jnumed.115.170456
46. Tade FI, Cohen MA, Styblo TM, Odewole OA, Holbrook AI, Newell MS, et al. Anti-3-18F-FACBC (18F-Fluciclovine) PET/CT of breast cancer: an exploratory study. *J Nucl Med.* (2016) 57:1357–63. doi: 10.2967/jnumed.115.171389
47. Ulaner GA, Goldman DA, Corben A, Lyashchenko SK, Gönen M, Lewis JS, et al. Prospective clinical trial of 18F-fluciclovine PET/CT for determining the response to neoadjuvant therapy in invasive ductal and invasive lobular breast cancers. *J Nucl Med.* (2017) 58:1037–42. doi: 10.2967/jnumed.116.183335
48. Baek S, Choi CM, Ahn SH, Lee JW, Gong G, Ryu JS, et al. Exploratory clinical trial of (4S)-4-(3-[18F]fluoropropyl)-L- glutamate for imaging xC- transporter using positron emission tomography in patients with non-small cell lung or breast cancer. *Clin Cancer Res.* (2012) 18:5427–37. doi: 10.1158/1078-0432.CCR-12-0214
49. Yang H, Jenni S, Colovic M, Merkens H, Poleschuk C, Rodrigo I, et al. 18F-5-Fluoroaminosuberic acid as a potential tracer to gauge oxidative stress in breast cancer models. *J Nucl Med.* (2017) 58:367–73. doi: 10.2967/jnumed.116.180661
50. Webster JM, Morton CA, Johnson BF, Yang H, Rishel MJ, Lee BD, et al. Functional imaging of oxidative stress with a novel PET imaging agent, 18f-5-fluoro-l-aminosuberic acid. *J Nucl Med.* (2014) 55:657–64. doi: 10.2967/jnumed.113.126664
51. Kole AC. Standardized uptake value and quantification of metabolism for breast cancer imaging with FDG and L-[1-11C]Tyrosine PET. *J Nucl Med.* (1997) 38:692–6.
52. Zhou R, Pantel AR, Li S, Lieberman BP, Ploessl K, Choi H, et al. [18F](2S,4R)4-fluoroglutamine PET detects glutamine pool size changes in triple-negative breast cancer in response to glutaminase inhibition. *Cancer Res.* (2017) 77:1476–84. doi: 10.1158/0008-5472.CAN-16-1945
53. Hanahan D, Weinberg RA. Hallmarks of cancer: the next generation. *Cell.* (2011) 144:646–674. doi: 10.1016/j.cell.2011.02.013
54. Kenny L. The use of novel PET tracers to image breast cancer biologic processes such as proliferation, DNA damage and repair, and angiogenesis. *J Nucl Med.* (2016) 57:89S−95S. doi: 10.2967/jnumed.115.157958
55. Mankoff DA, Shields AF, Link JM, Graham MM, Muzi M, Peterson LM, et al. Kinetic analysis of 2-[11C]thymidine PET imaging studies: validation studies. *J Nucl Med.* (1999) 40:614–24.
56. Mach RH, Dehdashti F, Wheeler KT. PET radiotracers for imaging the proliferative status of solid tumors. *PET Clin.* (2009) 4:1–15. doi: 10.1016/j.cpet.2009.04.012
57. Mankoff DA, Shields AF, Krohn KA. PET imaging of cellular proliferation. *Radiol Clin North Am.* (2005) 43:153–67. doi: 10.1016/j.rcl.2004.09.005
58. Shields AF, Mankoff DA, Link JM, Graham MM, Eary JF, Kozawa SM, et al. Carbon-11-thymidine and FDG to measure therapy response. *J Nucl Med.* (1998) 39:1757–62.
59. Shields AF, Mankoff D, Graham MM, Zheng M, Kozawa SM, Link JM, et al. Analysis of 2-carbon-11-thymidine blood metabolites in PET imaging. *J Nucl Med.* (1996) 37:290–6.
60. Smyczek-Gargya B, Fersis N, Dittmann H, Vogel U, Reischl G, Machulla HJ, et al. PET with [18F]fluorothymidine for imaging of primary breast cancer: a pilot study. *Eur J Nucl Med Mol Imaging.* (2004) 31:720–4. doi: 10.1007/s00259-004-1462-8

61. Chalkidou A, Landau DB, Odell EW, Cornelius VR, O'Doherty MJ, Marsden PK. Correlation between Ki-67 immunohistochemistry and 18F-Fluorothymidine uptake in patients with cancer: a systematic review and meta-analysis. *Eur J Cancer.* (2012) 48:3499–513. doi: 10.1016/j.ejca.2012.05.001
62. Bading JR, Shields AF. Imaging of cell proliferation: status and prospects. *J Nucl Med.* (2008) 49:64S−80S. doi: 10.2967/jnumed.107.046391
63. Li H, Liu Z, Yuan L, Fan K, Zhang Y, Cai W, et al. Radionuclide-based imaging of breast cancer: state of the art. *Cancers.* (2021) 13:5459. doi: 10.3390/cancers13215459
64. Linden HM, Dehdashti F. Novel methods and tracers for breast cancer imaging. *Semin Nucl Med.* (2013) 43:324–329. doi: 10.1053/j.semnuclmed.2013.02.003
65. Pio BS, Park CK, Pietras R, Hsueh WA, Satyamurthy N, Pegram MD, et al. Usefulness of 3′-[F-18]fluoro-3′-deoxythymidine with positron emission tomography in predicting breast cancer response to therapy. *Mol Imaging Biol.* (2006) 8:36–42. doi: 10.1007/s11307-005-0029-9
66. Kenny L, Coombes RC, Vigushin DM, Al-Nahhas A, Shousha S, Aboagye EO. Imaging early changes in proliferation at 1 week post chemotherapy: a pilot study in breast cancer patients with 3′-deoxy-3′-[18F]fluorothymidine positron emission tomography. *Eur J Nucl Med Mol Imaging.* (2007) 34:1339–47. doi: 10.1007/s00259-007-0379-4
67. López-Vega JM, Álvarez I, Antón A, Illarramendi JJ, Llombart A, Boni V García-Velloso MJ et al. Early imaging and molecular changes with neoadjuvant bevacizumab in stage ii/iii breast cancer. *Cancers.* (2021) 13:3511. doi: 10.3390/cancers13143511
68. Romine PE, Peterson LM, Kurland BF, Byrd DW, Novakova-Jiresova A, Muzi M, et al. 18 F-fluorodeoxyglucose (FDG) PET or 18 F-fluorothymidine (FLT) PET to assess early response to aromatase inhibitors (AI) in women with ER+ operable breast cancer in a window-of-opportunity study. *Breast Cancer Res.* (2021) 23:1–11. doi: 10.1186/S13058-021-01464-1
69. Su TP, Huang JS, Chang PH, Lui KW, Hsieh JCH, Ng SH, et al. Prospective comparison of early interim 18 F-FDG-PET with 18 F-FLT-PET for predicting treatment response and survival in metastatic breast cancer. *BMC Cancer.* (2021) 21:1–13. doi: 10.1186/S12885-021-08649-Z
70. Sun H, Sloan A, Mangner TJ, Vaishampayan U, Muzik O, Collins JM, et al. Imaging DNA synthesis with [18F]FMAU and positron emission tomography in patients with cancer. *Eur J Nucl Med Mol Imaging.* (2005) 32:15–22. doi: 10.1007/s00259-004-1713-8
71. Tehrani OS, Douglas KA, Lawhorn-Crews JM, Shields AF. Tracking cellular stress with labeled FMAU reflects changes in mitochondrial TK2. *Eur J Nucl Med Mol Imaging.* (2008) 35:1480–8. doi: 10.1007/s00259-008-0738-9
72. Al-Nabulsi I, Mach RH, Wang LM, Wallen CA, Keng PC, Sten K, et al. Effect of ploidy, recruitment, environmental factors, and tamoxifen treatment on the expression of sigma-2 receptors in proliferating and quiescent tumour cells. *Br J Cancer.* (1999) 81:925–33. doi: 10.1038/sj.bjc.6690789
73. Dehdashti F, Laforest R, Gao F, Shoghi KI, Aft RL, Nussenbaum B, et al. Assessment of cellular proliferation in tumors by PET using 18F-ISO-1. *J Nucl Med.* (2013) 54:350–7. doi: 10.2967/jnumed.112.111948
74. McDonald ES, Doot RK, Young AJ, Schubert EK, Tchou J, Pryma DA, et al. Breast cancer 18F-ISO-1 uptake as a marker of proliferation status. *J Nucl Med.* (2020) 61:665–70. doi: 10.2967/jnumed.119.232363
75. Karakashev SV, Reginato MJ. Progress toward overcoming hypoxia-induced resistance to solid tumor therapy. *Cancer Manag Res.* (2015) 7:253–64. doi: 10.2147/CMAR.S58285
76. Shannon AM, Bouchier-Hayes DJ, Condron CM, Toomey D. Tumour hypoxia, chemotherapeutic resistance and hypoxia-related therapies. *Cancer Treat Rev.* (2003) 29:297–307. doi: 10.1016/S0305-7372(03)00003-3
77. Fleming IN, Manavaki R, Blower PJ, West C, Williams KJ, Harris AL, et al. Imaging tumour hypoxia with positron emission tomography. *Br J Cancer.* (2015) 112:238–50. doi: 10.1038/bjc.2014.610
78. Valk PE, Mathis CA, Prados MD, Gilbert JC, Budinger TF. Hypoxia in human gliomas: demonstration by PET with fluorine-18- fluoromisonidazole. *J Nucl Med.* (1992) 33:2133–7.
79. Laking G, Price P. Radionuclide imaging of perfusion and hypoxia. *Eur J Nucl Med Mol Imaging.* (2010) 37:20–9. doi: 10.1007/s00259-010-1453-x
80. Rajendran JG, Mankoff DA, O'Sullivan F, Peterson LM, Schwartz DL, Conrad EU, et al. Hypoxia and glucose metabolism in malignant tumors: evaluation by [18F]Fluoromisonidazole and [18F]Fluorodeoxyglucose positron emission tomography imaging. *Clin Cancer Res.* (2004) 10:2245–52. doi: 10.1158/1078-0432.CCR-0688-3
81. Cheng J, Lei L, Xu J, Sun Y, Zhang Y, Wang X, et al. 18F-fluoromisonidazole PET/CT: a potential tool for predicting primary endocrine therapy resistance in breast cancer. *J Nucl Med.* (2013) 54:333–40. doi: 10.2967/jnumed.112.111963
82. Halmos GB, De Bruin LB, Langendijk JA, Van Der Laan BFAM, Pruim J, Steenbakkers RJHM. Head and neck tumor hypoxia imaging by 18F-fluoroazomycin- arabinoside (18F-FAZA)-PET: a review. *Clin Nucl Med.* (2014) 39:44–8. doi: 10.1097/RLU.0000000000000286
83. Lopci E, Grassi I, Chiti A, Nanni C, Cicoria G, Toschi L, et al. PET radiopharmaceuticals for imaging of tumor hypoxia: a review of the evidence. *Am J Nucl Med Mol Imaging.* (2014) 4:365–84.
84. Lohith TG, Kudo T, Demura Y, Umeda Y, Kiyono Y, Fujibayashi Y, et al. Pathophysiologic correlation between 62Cu-ATSM and 18F-FDG in lung cancer. *J Nucl Med.* (2009) 50:1948–53. doi: 10.2967/jnumed.109.069021
85. Dehdashti F, Grigsby PW, Lewis JS, Laforest R, Siegel BA, Welch MJ. Assessing tumor hypoxia in cervical cancer by PET with 60Cu- labeled diacetyl-bis(N4-methylthiosemicarbazone). *J Nucl Med.* (2008) 49:201–5. doi: 10.2967/jnumed.107.048520
86. Dietz DW, Dehdashti F, Grigsby PW, Malyapa RS, Myerson RJ, Picus J, et al. Tumor hypoxia detected by positron emission tomography with 60Cu-ATSM as a predictor of response and survival in patients undergoing neoadjuvant chemoradiotherapy for rectal carcinoma: a pilot study. *Dis Colon Rectum.* (2008) 51:1641–8. doi: 10.1007/s10350-008-9420-3
87. Tateishi K, Tateishi U, Sato M, Yamanaka S, Kanno H, Murata H, et al. Application of 62Cu-diacetyl-bis (N4- methylthiosemicarbazone) PET imaging to predict highly malignant tumor grades and hypoxia-inducible factor-1α expression in patients with glioma. *Am J Neuroradiol.* (2013) 34:92–9. doi: 10.3174/ajnr.A3159
88. Hu M, Xing L, Mu D, Yang W, Yang G, Kong L, et al. Hypoxia imaging with 18F-fluoroerythronitroimidazole integrated PET/CT and immunohistochemical studies in non-small cell lung cancer. *Clin Nucl Med.* (2013) 38:591–6. doi: 10.1097/RLU.0b013e318279fd3d
89. Beppu T, Terasaki K, Sasaki T, Fujiwara S, Matsuura H, Ogasawara K, et al. Standardized uptake value in high uptake area on positron emission tomography with 18F-FRP170 as a hypoxic cell tracer correlates with intratumoral oxygen pressure in glioblastoma. *Mol Imaging Biol.* (2014) 16:127–35. doi: 10.1007/s11307-013-0670-7
90. Zegers CML, Van Elmpt W, Wierts R, Reymen B, Sharifi H, Öllers MC, et al. Hypoxia imaging with [18F]HX4 PET in NSCLC patients: defining optimal imaging parameters. *Radiother Oncol.* (2013) 109:58–64. doi: 10.1016/j.radonc.2013.08.031
91. Aurilio G, Disalvatore D, Pruneri G, Bagnardi V, Viale G, Curigliano G, et al. A meta-analysis of oestrogen receptor, progesterone receptor and human epidermal growth factor receptor 2 discordance between primary breast cancer and metastases. *Eur J Cancer.* (2014) 50:277–89. doi: 10.1016/j.ejca.2013.10.004
92. Zoubina EV, Smith PG. Expression of estrogen receptors α and β by sympathetic ganglion neurons projecting to the proximal urethra of female rats. *J Urol.* (2003) 169:382–5. doi: 10.1016/S0022-5347(05)64132-8
93. Pettersson K, Gustafsson JA. Role of estrogen receptor beta in estrogen action. *Annu Rev Physiol.* (2001) 63:165–92. doi: 10.1146/annurev.physiol.63.1.165
94. Seimbille Y, Rousseau J, Bénard F, Morin C, Ali H, Avvakumov G, et al. 18F-labeled difluoroestradiols: preparation and preclinical evaluation as estrogen receptor-binding radiopharmaceuticals. *Steroids.* (2002) 67:765–75. doi: 10.1016/S0039-128X(02)00025-9
95. Sasaki M, Fukumura T, Kuwabara Y, Yoshida T, Nakagawa M, Ichiya Y, et al. Biodistribution and breast tumor uptake of 16α-[18F]-fluoro-17 β-estradiol in rat. *Ann Nucl Med.* (2000) 14:127–30. doi: 10.1007/BF02988592
96. Iqbal R, Yaqub M, Oprea-Lager DE, Liu Y, Luik AM, Beelan A, et al. Biodistribution of 18F-FES in patients with metastatic ER+ breast cancer undergoing treatment with Rintodestrant (G1T48), a novel selective estrogen receptor degrader. *J Nucl Med.* (2021). doi: 10.2967/jnumed.121.262500 [Epub ahead of print].

97. Mankoff DA, Tewson TJ, Eary JF. Analysis of blood clearance and labeled metabolites for the estrogen receptor tracer [F-18]-16α-Fluorestradiol (FES). *Nucl Med Biol.* (1997) 24:341–8. doi: 10.1016/S0969-8051(97)00002-4
98. Mintun MA, Welch MJ, Siegel BA, Mathias CJ, Brodack JW, McGuire AH, et al. Breast cancer: PET imaging of estrogen receptors. *Radiology.* (1988) 169:45–8. doi: 10.1148/radiology.169.1.3262228
99. Kurland BF, Wiggins JR, Coche A, Fontan C, Bouvet Y, Webner P, et al. Whole-body characterization of estrogen receptor status in metastatic breast cancer with 16α-18F-Fluoro-17β-estradiol positron emission tomography: meta-analysis and recommendations for integration into clinical applications. *Oncologist.* (2020) 25:835–44. doi: 10.1634/theoncologist.2019-0967
100. Boers J, Giatagana K, Schröder CP, Hospers GAP, de Vries EFJ, Glaudemans AWJM. Image quality and interpretation of [18F]-FES-PET: is there any effect of food intake? *Diagnostics.* (2020) 10:756. doi: 10.3390/diagnostics10100756
101. Venema CM, Apollonio G, Hospers GAP, Schröder CP, Dierckx RAJO, De Vries EFJ, et al. Recommendations and technical aspects of 16α-[18F]Fluoro-17β-Estradiol PET to image the estrogen receptor *in vivo*. *Clin Nucl Med.* (2016) 41:844–51. doi: 10.1097/RLU.0000000000001347
102. Liu C, Gong C, Liu S, Zhang Y, Zhang Y, Xu X, et al. 18 F-FES PET/CT influences the staging management of patients with newly diagnosed estrogen receptor-positive breast cancer: a retrospective comparative study with 18 F-FDG PET/CT. *Oncologist.* (2019) 24:e1277–85. doi: 10.1634/theoncologist.2019-0096
103. Ulaner GA, Jhaveri K, Chandarlapaty S, Hatzoglou V, Riedl CC, Lewis JS, et al. Head-to-head evaluation of 18F-FES and 18F-FDG PET/CT in metastatic invasive lobular breast cancer. *J Nucl Med.* (2021) 62:326–31. doi: 10.2967/jnumed.120.247882
104. Boers J, Loudini N, Brunsch CL, Koza SA, de Vries EFJ, Glaudemans AWJM, et al. Value of 18 F-FES PET in solving clinical dilemmas in breast cancer patients: a retrospective study. *J Nucl Med.* (2021) 62:1214–20. doi: 10.2967/jnumed.120.256826
105. Peterson LM, Kurland BF, Schubert EK, Link JM, Gadi VK, Specht JM, et al. A phase 2 study of 16α-[18F]-fluoro-17β-estradiol positron emission tomography (FES-PET) as a marker of hormone sensitivity in metastatic breast cancer (MBC). *Mol Imaging Biol.* (2014) 16:431–40. doi: 10.1007/s11307-013-0699-7
106. Linden HM, Kurland BF, Peterson LM, Schubert EK, Gralow JR, Specht JM, et al. Fluoroestradiol positron emission tomography reveals differences in pharmacodynamics of aromatase inhibitors, tamoxifen, and fulvestrant in patients with metastatic breast cancer. *Clin Cancer Res.* (2011) 17:4799–805. doi: 10.1158/1078-0432.CCR-10-3321
107. van Kruchten M, Glaudemans AWJM, de Vries EFJ, Schröder CP, de Vries EGE, Hospers GAP. Positron emission tomography of tumour [18F]fluoroestradiol uptake in patients with acquired hormone-resistant metastatic breast cancer prior to oestradiol therapy. *Eur J Nucl Med Mol Imaging.* (2015) 42:1674–81. doi: 10.1007/s00259-015-3107-5
108. Gong C, Yang Z, Sun Y, Zhang J, Zheng C, Wang L, et al. A preliminary study of 18F-FES PET/CT in predicting metastatic breast cancer in patients receiving docetaxel or fulvestrant with docetaxel. *Sci Rep.* (2017) 7:1–10. doi: 10.1038/s41598-017-06903-8
109. Dehdashti F, Mortimer JE, Trinkaus K, Naughton MJ, Ellis M, Katzenellenbogen JA, et al. PET-based estradiol challenge as a predictive biomarker of response to endocrine therapy in women with estrogen-receptor-positive breast cancer. *Breast Cancer Res Treat.* (2009) 113:509–17. doi: 10.1007/s10549-008-9953-0
110. Evangelista L, Vittoria Dieci M, Guarneri V, Franco Conte P. 18F-fluoroestradiol positron emission tomography in breast cancer patients: systematic review of the literature & meta-analysis. *Curr Radiopharm.* (2016) 9:244–57. doi: 10.2174/1874471009666161019144950
111. Yang Z, Sun Y, Xue J, Yao Z, Xu J, Cheng J, et al. Can positron emission tomography/computed tomography with the dual tracers fluorine-18 fluoroestradiol and fluorodeoxyglucose predict neoadjuvant chemotherapy response of breast cancer? -A pilot study. *PLoS ONE.* (2013) 8:e78192. doi: 10.1371/journal.pone.0078192
112. Paquette M, Lavallée É, Phoenix S, Ouellet R, Senta H, Van Lier JE, et al. Improved estrogen receptor assessment by PET using the novel radiotracer 18 F-4FMFES in estrogen receptor–positive breast cancer patients: an ongoing phase II clinical trial. *J Nucl Med.* (2018) 59:197–203. doi: 10.2967/jnumed.117.194654
113. Xu D, Zhuang R, You L, Guo Z, Wang X, Peng C, et al. 18 F–labeled estradiol derivative for targeting estrogen receptor-expressing breast cancer. *Nucl Med Biol.* (2018) 59:48–55. doi: 10.1016/j.nucmedbio.2018.01.003
114. Hammond MEH, Hayes DF, Dowsett M, Allred DC, Hagerty KL, Badve S, et al. American Society of Clinical oncology/college of American Pathologists guideline recommendations for immunohistochemical testing of estrogen and progesterone receptors in breast cancer. *Arch Pathol Lab Med.* (2010) 134:907–22. doi: 10.5858/134.7.e48
115. McKenna NJ, O'Malley BW. Combinatorial control of gene expression by nuclear receptors and coregulators. *Cell.* (2002) 108:465–74. doi: 10.1016/S0092-8674(02)00641-4
116. Cunha S, Gano L, Ribeiro Morais G, Thiemann T, Oliveira MC. Progesterone receptor targeting with radiolabelled steroids: an approach in predicting breast cancer response to therapy. *J Steroid Biochem Mol Biol.* (2013) 137:223–41. doi: 10.1016/j.jsbmb.2013.04.003
117. Natrajan R, Weigelt B, Mackay A, Geyer FC, Grigoriadis A, Tan DSP, et al. An integrative genomic and transcriptomic analysis reveals molecular pathways and networks regulated by copy number aberrations in basal-like, HER2 and luminal cancers. *Breast Cancer Res Treat.* (2010) 121:575–89. doi: 10.1007/s10549-009-0501-3
118. Viale G, Regan MM, Maiorano E, Mastropasqua MG, Dell'Orto P, Rasmussen BB, et al. Prognostic and predictive value of centrally reviewed expression of estrogen and progesterone receptors in a randomized trial comparing letrozole and tamoxifen adjuvant therapy for postmenopausal early breast cancer: BIG 1-98. *J Clin Oncol.* (2007) 25:3846–52. doi: 10.1200/JCO.2007.11.9453
119. Clarke RB, Anderson E, Howell A. Steroid receptors in human breast cancer. *Trends Endocrinol Metab.* (2004) 15:316–23. doi: 10.1016/j.tem.2004.07.004
120. Pomper MG, Katzenellenbogen JA, Welch MJ, Brodack JW, Mathias CJ. 21-[18F]Fluoro-16α-ethyl-19-norprogesterone: synthesis and target tissue selective uptake of a progestin receptor based radiotracer for positron emission tomography. *J Med Chem.* (1988) 31:1360–3. doi: 10.1021/jm00402a019
121. Dehdashti F, McGuire AH, Van Brocklin HF, Siegel BA, Andriole DP, Griffeth LK, et al. Assessment of 21-[18F]fluoro-16α-ethyl-19-norprogesterone as a positron-emitting radiopharmaceutical for the detection of progestin receptors in human breast carcinomas. *J Nucl Med.* (1991) 32:1532–7.
122. Verhagen A, Studeny M, Luurtsema G, Visser GM, De Goeij CCJ, Sluyser M, et al. Metabolism of a [18F]fluorine labeled progestin (21 -[18F]fluoro-16α -ethyl-19-norprogesterone) in humans: a clue for future investigations. *Nucl Med Biol.* (1994) 21:941–52. doi: 10.1016/0969-8051(94)90083-3
123. Choe YS, Bonasera TA, Chi DY, Welch MJ, Katzenellenbogen JA. 6α-[18F]Fluoroprogesterone: synthesis via halofluorination-oxidation, receptor binding and tissue distribution. *Nucl Med Biol.* (1995) 22:635–42. doi: 10.1016/0969-8051(94)00142-7
124. Buckman BO, Bonasera TA, Kirschbaum KS, Welch MJ, Katzenellenbogen JA. Fluorine-18-labeled progestin 16α, 17α-dioxolanes: development of high-affinity ligands for the progesterone receptor with high *in vivo* target site selectivity. *J Med Chem.* (1995) 38:328–37. doi: 10.1021/jm00002a014
125. Vijaykumar D, Mao W, Kirschbaum KS, Katzenellenbogen JA. An efficient route for the preparation of a 21-fluoro progestin-16α,17α-dioxolane, a high-affinity ligand for PET imaging of the progesterone receptor. *J Org Chem.* (2002) 67:4904–10. doi: 10.1021/jo020190r
126. Dehdashti F, Laforest R, Gao F, Aft RL, Dence CS, Zhou D, et al. Assessment of progesterone receptors in breast carcinoma by PET with 21- 18F-fluoro-16α,17α-[(R)-(1′-α- furylmethylidene) dioxy]-19-norpregn-4-ene-3,20-dione. *J Nucl Med.* (2012) 53:363–70. doi: 10.2967/jnumed.111.098319
127. Fowler AM, Chan SR, Sharp TL, Fettig NM, Zhou D, Dence CS, et al. Small-animal PET of steroid hormone receptors predicts tumor response to endocrine therapy using a preclinical model of breast cancer. *J Nucl Med.* (2012) 53:1119–26. doi: 10.2967/jnumed.112.103465
128. Dehdashti F, Wu N, Ma CX, Naughton MJ, Katzenellenbogen JA, Siegel BA. Association of PET-based estradiol-challenge test for breast cancer progesterone receptors with response to endocrine therapy. *Nat Commun.* (2021) 12:1–9. doi: 10.1038/s41467-020-20814-9

129. Harari D, Yarden Y. Molecular mechanisms underlying ErbB2/HER2 action in breast cancer. *Oncogene.* (2000) 19:6102–14. doi: 10.1038/sj.onc.1203973
130. Kreutzfeldt J, Rozeboom B, Dey N, De P. The trastuzumab era: current and upcoming targeted HER2+ breast cancer therapies. *Am J Cancer Res.* (2020) 10:1045–67.
131. Velikyan I, Schweighöfer P, Feldwisch J, Seemann J, Frejd FY, Lindman H, et al. Diagnostic HER2-binding radiopharmaceutical, [68Ga]Ga-ABY-025, for routine clinical use in breast cancer patients. *Am J Nucl Med Mol Imaging.* (2019) 9:12–23.
132. Fumagalli C, Barberis M. Breast cancer heterogeneity. *Diagnostics.* (2021) 11:1555. doi: 10.3390/diagnostics11091555
133. Sekar TV, Dhanabalan A, Paulmurugan R. Imaging cellular receptors in breast cancers: an overview. *Curr Pharm Biotechnol.* (2011) 12:508–27. doi: 10.2174/138920111795164039
134. Carter P, Presta L, Gorman CM, Ridgway JBB, Henner D, Wong WLT, et al. Humanization of an anti-p185HER2 antibody for human cancer therapy. *Proc Natl Acad Sci USA.* (1992) 89:4285–9. doi: 10.1073/pnas.89.10.4285
135. Chang AJ, DeSilva R, Jain S, Lears K, Rogers B, Lapi S. 89Zr-radiolabeled trastuzumab imaging in orthotopic and metastatic breast tumors. *Pharmaceuticals.* (2012) 5:79–93. doi: 10.3390/ph5010079
136. Dijkers EC, Oude Munnink TH, Kosterink JG, Brouwers AH, Jager PL, De Jong JR, et al. Biodistribution of 89 Zr-trastuzumab and PET imaging of HER2-positive lesions in patients with metastatic breast cancer. *Clin Pharmacol Ther.* (2010) 87:586–92. doi: 10.1038/clpt.2010.12
137. Laforest R, Lapi SE, Oyama R, Bose R, Tabchy A, Marquez-Nostra BV, et al. [89Zr]Trastuzumab: evaluation of radiation dosimetry, safety, and optimal imaging parameters in women with HER2-positive breast cancer. *Mol Imaging Biol.* (2016) 18:952–9. doi: 10.1007/s11307-016-0951-z
138. Gebhart G, Lamberts LE, Wimana Z, Garcia C, Emonts P, Ameye L, et al. Molecular imaging as a tool to investigate heterogeneity of advanced HER2-positive breast cancer and to predict patient outcome under trastuzumab emtansine (T-DM1): the ZEPHIR trial. *Ann Oncol.* (2016) 27:619–24. doi: 10.1093/annonc/mdv577
139. Bensch F, Brouwers AH, Lub-de Hooge MN, de Jong JR, van der Vegt B, Sleijfer S, et al. 89Zr-trastuzumab PET supports clinical decision making in breast cancer patients, when HER2 status cannot be determined by standard work up. *Eur J Nucl Med Mol Imaging.* (2018) 45:2300–6. doi: 10.1007/s00259-018-4099-8
140. Tamura K, Kurihara H, Yonemori K, Tsuda H, Suzuki J, Kono Y, et al. 64Cu-DOTA-trastuzumab PET imaging in patients with HER2-positive breast cancer. *J Nucl Med.* (2013) 54:1869–75. doi: 10.2967/jnumed.112.118612
141. Mortimer JE, Bading JR, Colcher DM, Conti PS, Frankel PH, Carroll MI, et al. Functional imaging of human epidermal growth factor receptor 2-positive metastatic breast cancer using 64Cu-DOTA-trastuzumab PET. *J Nucl Med.* (2014) 55:23–9. doi: 10.2967/jnumed.113.122630
142. Carrasquillo JA, Morris PG, Humm JL, Smith-Jones PM, Beylergil V, Akhurst T, et al. Copper-64 trastuzumab PET imaging: a reproducibility study. *Q J Nucl Med Mol Imaging.* (2019) 63:191–8. doi: 10.23736/S1824-4785.16.02867-3
143. Baum RP, Prasad V, Müller D, Schuchardt C, Orlova A, Wennborg A, et al. Molecular imaging of HER2-expressing malignant tumors in breast cancer patients using synthetic 111In- or 68Ga-labeled Affibody molecules. *J Nucl Med.* (2010) 51:892–7. doi: 10.2967/jnumed.109.073239
144. Sörensen J, Velikyan I, Sandberg D, Wennborg A, Feldwisch J, Tolmachev V, et al. Measuring HER2-receptor expression in metastatic breast cancer using [68Ga]ABY-025 Affibody PET/CT. *Theranostics.* (2016) 6:262–71. doi: 10.7150/thno.13502
145. Sandström M, Lindskog K, Velikyan I, Wennborg A, Feldwisch J, Sandberg D, et al. Biodistribution and radiation dosimetry of the anti-HER2 Affibody molecule 68Ga-ABY-025 in breast cancer patients. *J Nucl Med.* (2016) 57:867–71. doi: 10.2967/jnumed.115.169342
146. Sandberg D, Tolmachev V, Velikyan I, Olofsson H, Wennborg A, Feldwisch J, et al. Intra-image referencing for simplified assessment of HER2-expression in breast cancer metastases using the Affibody molecule ABY-025 with PET and SPECT. *Eur J Nucl Med Mol Imaging.* (2017) 44:1337–46. doi: 10.1007/s00259-017-3650-3
147. Su CY, Li JQ, Zhang LL, Wang H, Wang FH, Tao YW, et al. The biological functions and clinical applications of integrins in cancers. *Front Pharmacol.* (2020) 11:1435. doi: 10.3389/fphar.2020.579068
148. Madu CO, Wang S, Madu CO, Lu Y. Angiogenesis in breast cancer progression, diagnosis, and treatment. *J Cancer.* (2020) 11:4474–94. doi: 10.7150/jca.44313
149. Yousefi H, Vatanmakanian M, Mahdiannasser M, Mashouri L, Alahari NV, Monjezi MR, et al. Understanding the role of integrins in breast cancer invasion, metastasis, angiogenesis, and drug resistance. *Oncogene.* (2021) 40:1043–63. doi: 10.1038/s41388-020-01588-2
150. Goldfarb SB, Dickler MN. Bevacizumab in metastatic breast cancer: when may it be used? *Ther Adv Med Oncol.* (2011) 3:85–93. doi: 10.1177/1758834010397627
151. Laudicella R, Quartuccio N, Argiroffi G, Alongi P, Baratto L, Califaretti E, et al. Unconventional non-amino acidic PET radiotracers for molecular imaging in gliomas. *Eur J Nucl Med Mol Imaging.* (2021) 48:3925–39. doi: 10.1007/s00259-021-05352-w
152. Beer AJ, Kessler H, Wester H-J, Schwaiger M. PET imaging of integrin αVβ3 expression. *Theranostics.* (2012) 1:48–57. doi: 10.7150/thno/v01p0048
153. Kazmierczak PM, Todica A, Gildehaus FJ, Hirner-Eppeneder H, Brendel M, Eschbach RS, et al. 68Ga-TRAP-(RGD)3 hybrid imaging for the *in vivo* monitoring of αvβ3-integrin expression as biomarker of anti-angiogenic therapy effects in experimental breast cancer. *PLoS ONE.* (2016) 11:e168248. doi: 10.1371/journal.pone.0168248
154. Beer AJ, Niemeyer M, Carlsen J, Sarbia M, Nahrig J, Watzlowik P, et al. Patterns of αvβ3 expression in primary and metastatic human breast cancer as shown by 18F-galacto-RGD PET. *J Nucl Med.* (2008) 49:255–9. doi: 10.2967/jnumed.107.045526
155. Baum RP, Kulkarni HR, Müller D, Satz S, Danthi N, Kim YS, et al. First-in-human study demonstrating tumor-angiogenesis by PET/CT imaging with 68Ga-NODAGA-THERANOST, a high-affinity peptidomimetic for αvβ3 integrin receptor targeting. *Cancer Biother Radiopharm.* (2015) 30:152–9. doi: 10.1089/cbr.2014.1747
156. Kenny LM, Al-Nahhas A, Aboagye EO. Novel PET biomarkers for breast cancer imaging. *Nucl Med Commun.* (2011) 32:333–5. doi: 10.1097/MNM.0b013e32834471ff
157. Kenny LM, Coombes RC, Oulie I, Contractor KB, Miller M, Spinks TJ, et al. Phase I trial of the positron-emitting Arg-Gly-Asp (RGD) peptide radioligand 18F-AH111585 in breast cancer patients. *J Nucl Med.* (2008) 49:879–86. doi: 10.2967/jnumed.107.049452
158. Tomasi G, Kenny L, Mauri F, Turkheimer F, Aboagye EO. Quantification of receptor-ligand binding with [18F]fluciclatide in metastatic breast cancer patients. *Eur J Nucl Med Mol Imaging.* (2011) 38:2186–97. doi: 10.1007/s00259-011-1907-9
159. Iagaru A, Mosci C, Shen B, Chin FT, Mittra E, Telli ML, et al. 18F-FPPRGD2 PET/CT: pilot phase evaluation of breast cancer patients. *Radiology.* (2014) 273:549–59. doi: 10.1148/radiol.14140028
160. Gaykema SBM, Brouwers AH, Hooge MNL De, Pleijhuis RG, Timmer-Bosscha H, Pot L, et al. 89Zr-bevacizumab PET imaging in primary breast cancer. *J Nucl Med.* (2013) 54:1014–8. doi: 10.2967/jnumed.112.117218
161. Glunde K, Bhujwalla ZM. Metabolic tumor imaging using magnetic resonance spectroscopy. *Semin Oncol.* (2011) 38:26–41. doi: 10.1053/j.seminoncol.2010.11.001
162. Cheng M, Bhujwalla ZM, Glunde K. Targeting phospholipid metabolism in cancer. *Front Oncol.* (2016) 6:266. doi: 10.3389/fonc.2016.00266
163. Liberini V, Morand GB, Rupp NJ, Orita E, Deandreis D, Broglie Däppen M, et al. Histopathological features of parathyroid adenoma and 18F-choline uptake in PET/MR of primary hyperparathyroidism. *Clin Nucl Med.* (2022) 47:101–7. doi: 10.1097/RLU.0000000000003987
164. Aboagye EO, Bhujwalla ZM. Malignant transformation alters membrane choline phospholipid metabolism of human mammary epithelial cells. *Cancer Res.* (1999) 59:80–4.
165. Wang R, Shen G, Huang M, Tian R. The diagnostic role of 18F-choline, 18F-fluciclovine and 18F-PSMA PET/CT in the detection of prostate cancer with biochemical recurrence: a meta-analysis. *Front Oncol.* (2021) 11:684629. doi: 10.3389/fonc.2021.684629
166. Vadrucci M, Gilardi L, Grana CM. Breast cancer incidentally detected by 18F-choline PET/CT in a patient with recurrent prostate carcinoma. *Clin Nucl Med.* (2016) 41:892–3. doi: 10.1097/rlu.0000000000001350
167. Contractor KB, Kenny LM, Stebbing J, Al-Nahhas A, Palmieri C, Sinnett D, et al. [11C]choline positron emission tomography in estrogen receptor-positive breast cancer. *Clin Cancer Res.* (2009) 15:5503–10. doi: 10.1158/1078-0432.CCR-09-0666

168. Kenny LM, Contractor KB, Hinz R, Stebbing J, Palmieri C, Jiang J, et al. Reproducibility of [11C]choline-positron emission tomography and effect of trastuzumab. *Clin Cancer Res.* (2010) 16:4236–45. doi: 10.1158/1078-0432.CCR-10-0468
169. Kwee SA, Coel MN. Detection of synchronous primary breast and prostate cancer by F-18 fluorocholine PET/CT. *Clin Nucl Med.* (2010) 35:128–9. doi: 10.1097/RLU.0b013e3181c7c019
170. Ahmad Saad FF, Zakaria MH, Appanna B. PET/CT analysis of 21 patients with breast cancer: physiological distribution of 18 F-choline and diagnostic pitfalls. *J Int Med Res.* (2018) 46:3138–48. doi: 10.1177/0300060518773019
171. Hofman MS, Hicks RJ, Maurer T, Eiber M. Prostate-specific membrane antigen PET: clinical utility in prostate cancer, normal patterns, pearls, and pitfalls. *Radiographics.* (2018) 38:200–17. doi: 10.1148/rg.2018170108
172. Noss KR, Wolfe SA, Grimes SR. Upregulation of prostate specific membrane antigen/folate hydrolase transcription by an enhancer. *Gene.* (2002) 285:247–56. doi: 10.1016/S0378-1119(02)00397-9
173. Roberto ASF, Amir T, Sheikhbahaei S, Harvey SC, Javadi MS, Solnes LB, et al. Imaging of nonprostate cancers using PSMA-targeted radiotracers: rationale, current state of the field, and a call to arms. *J Nucl Med.* (2018) 59:871–7. doi: 10.2967/jnumed.117.203570
174. Wernicke AG, Varma S, Greenwood EA, Christos PJ, Chao KSC, Liu H, et al. Prostate-specific membrane antigen expression in tumor-associated vasculature of breast cancers. *APMIS.* (2014) 122:482–9. doi: 10.1111/apm.12195
175. Polverari G, Ceci F, Calderoni L, Cervati V, Farolfi A, Castellucci P, et al. Male breast cancer detected by 68 Ga-PSMA-11 PET/CT in a patient with prostate cancer with pelvic lymph node metastasis. *Clin Genitourin Cancer.* (2019) 17:154–6. doi: 10.1016/J.CLGC.2018.11.020
176. Daglioz Gorur G, Hekimsoy T, Isgoren S. Re: false positive uptake in bilateral gynecomastia on 68Ga-PSMA PET/CT scan. *Clin Nucl Med.* (2018) 43:785. doi: 10.1097/RLU.0000000000002086
177. Kumar R, Mittal BR, Bhattacharya A, Singh H, Singh SK. Synchronous detection of male breast cancer and prostatic cancer in a patient with suspected prostatic carcinoma on 68Ga-PSMA PET/CT imaging. *Clin Nucl Med.* (2018) 43:431–2. doi: 10.1097/RLU.0000000000002063
178. Malik D, Kumar R, Mittal BR, Singh H, Bhattacharya A, Singh SK. 68Ga-labeled PSMA uptake in nonprostatic malignancies: has the time come to remove "pS" from PSMA? *Clin Nucl Med.* (2018) 43:529–32. doi: 10.1097/RLU.0000000000002103
179. Medina-Ornelas SS, García-Pérez FO, Medel-Gamez C, Paredes-Amoroto E. Metástasis cerebral única, evidenciada mediante PET/TC con 68Ga-PSMA en recurrencia de cáncer de mama. *Rev Esp Med Nucl Imagen Mol.* (2018) 37:61–2. doi: 10.1016/j.remn.2017.04.004
180. Parihar AS, Mittal BR, Sood A, Basher RK, Singh G. 68Ga-prostate-specific membrane antigen PET/CT and 18F-FDG PET/CT of primary signet ring cell breast adenocarcinoma. *Clin Nucl Med.* (2018) 43:e414–6. doi: 10.1097/RLU.0000000000002265
181. Passah A, Arora S, Damle NA, Tripathi M, Bal C, Subudhi TK, et al. 68Ga-prostate-specific membrane antigen PET/CT in triple-negative breast cancer. *Clin Nucl Med.* (2018) 43:460–1. doi: 10.1097/RLU.0000000000002071
182. Tolkach Y, Gevensleben H, Bundschuh R, Koyun A, Huber D, Kehrer C, et al. Prostate-specific membrane antigen in breast cancer: a comprehensive evaluation of expression and a case report of radionuclide therapy. *Breast Cancer Res Treat.* (2018) 169:447–55. doi: 10.1007/s10549-018-4717-y
183. Sasikumar A, Joy A, Nair BP, Pillai MRA, Madhavan J. False positive uptake in bilateral gynecomastia on 68Ga-PSMA PET/CT scan. *Clin Nucl Med.* (2017) 42:e412–4. doi: 10.1097/RLU.0000000000001742
184. Sathekge M, Modiselle M, Vorster M, Mokgoro N, Nyakale N, Mokaleng B, et al. 68Ga-PSMA imaging of metastatic breast cancer. *Eur J Nucl Med Mol Imaging.* (2015) 42:1482–3. doi: 10.1007/s00259-015-3066-x
185. Sathekge M, Lengana T, Modiselle M, Vorster M, Zeevaart JR, Maes A, et al. 68Ga-PSMA-HBED-CC PET imaging in breast carcinoma patients. *Eur J Nucl Med Mol Imaging.* (2017) 44:689–94. doi: 10.1007/s00259-016-3563-6
186. Liberini V, Mariniello A, Righi L, Capozza M, Delcuratolo MD, Terreno E, et al. Nsclc biomarkers to predict response to immunotherapy with checkpoint inhibitors (Ici): from the cells to *in vivo* images. *Cancers.* (2021) 13:4543. doi: 10.3390/cancers13184543
187. Tolba MF, Santa-Maria CA, Albini A, Chimusa ER, Al-Ramadi BK, Tolaney SM. Editorial: immunotherapy as an evolving approach for the treatment of breast cancer. *Front Oncol.* (2021) 11:752689. doi: 10.3389/fonc.2021.752689
188. Emens LA, Adams S, Cimino-Mathews A, Disis ML, Gatti-Mays ME, Ho AY, et al. Society for Immunotherapy of Cancer (SITC) clinical practice guideline on immunotherapy for the treatment of breast cancer. *J Immunother Cancer.* (2021) 9:e002597. doi: 10.1136/jitc-2021-002597
189. Liberini V, Laudicella R, Capozza M, Huellner MW, Burger IA, Baldari S, et al. The future of cancer diagnosis, treatment and surveillance: a systemic review on immunotherapy and immuno-pet radiotracers. *Molecules.* (2021) 26:2201. doi: 10.3390/molecules26082201
190. Bensch F, van der Veen EL, Lub-de Hooge MN, Jorritsma-Smit A, Boellaard R, Kok IC, et al. 89Zr-atezolizumab imaging as a non-invasive approach to assess clinical response to PD-L1 blockade in cancer. *Nat Med.* (2018) 24:1852–8. doi: 10.1038/s41591-018-0255-8
191. Barrett RL, Pure E. Cancer-associated fibroblasts and their influence on tumor immunity and immunotherapy. *Elife.* (2020) 9:1–20. doi: 10.7554/ELIFE.57243
192. Sliker BH, Campbell PM. Fibroblasts influence the efficacy, resistance, and future use of vaccines and immunotherapy in cancer treatment. *Vaccines.* (2021) 9:634. doi: 10.3390/vaccines9060634
193. Sollini M, Kirienko M, Gelardi F, Fiz F, Gozzi N, Chiti A. State-of-the-art of FAPI-PET imaging: a systematic review and meta-analysis. *Eur J Nucl Med Mol Imaging.* (2021) 48:4396–414. doi: 10.1007/s00259-021-05475-0
194. Loktev A, Lindner T, Mier W, Debus J, Altmann A, Jäger D, et al. A tumor-imaging method targeting cancer-associated fibroblasts. *J Nucl Med.* (2018) 59:1423–9. doi: 10.2967/jnumed.118.210435
195. Kratochwil C, Flechsig P, Lindner T, Abderrahim L, Altmann A, Mier W, et al. 68Ga-FAPI PET/CT: tracer uptake in 28 different kinds of cancer. *J Nucl Med.* (2019) 60:801–5. doi: 10.2967/jnumed.119.227967
196. Giesel F, Flechsig P, Labidi A, Rathke H, Rathke M, Debus J, et al. Intensity of tracer-uptake in FAPI-PET/CT in different kinds of cancer. *J Nucl Med.* (2019) 60:289. Available online at: https://jnm.snmjournals.org/content/60/supplement_1/289
197. Calais J, Mona CE. Will FAPI PET/CT replace FDG PET/CT in the next decade? Point—an important diagnostic, phenotypic, and biomarker role. *Am J Roentgenol.* (2021) 216:305–6. doi: 10.2214/AJR.20.24302
198. Elboga U, Sahin E, Kus T, Cayirli YB, Aktas G, Uzun E, et al. Superiority of 68Ga-FAPI PET/CT scan in detecting additional lesions compared to 18FDG PET/CT scan in breast cancer. *Ann Nucl Med.* (2021) 35:1321–31. doi: 10.1007/s12149-021-01672-x
199. Kömek H, Can C, Güzel Y, Oruç Z, Gündogan C, Yildirim ÖA, et al. 68Ga-FAPI-04 PET/CT, a new step in breast cancer imaging: a comparative pilot study with the 18F-FDG PET/CT. *Ann Nucl Med.* (2021) 35:744–52. doi: 10.1007/s12149-021-01616-5
200. Watabe T, Liu Y, Kaneda-Nakashima K, Shirakami Y, Lindner T, Ooe K, et al. Theranostics targeting fibroblast activation protein in the tumor stroma: 64Cu- And 225Ac-labeled FAPI-04 in pancreatic cancer xenograft mouse models. *J Nucl Med.* (2020) 61:563–9. doi: 10.2967/jnumed.119.233122
201. Kuyumcu S, Kovan B, Sanli Y, Buyukkaya F, Has Simsek D, Özkan ZG, et al. Safety of fibroblast activation protein-targeted radionuclide therapy by a low-dose dosimetric approach using 177Lu-FAPI04. *Clin Nucl Med.* (2021) 46:641–6. doi: 10.1097/RLU.0000000000003667
202. Eryilmaz K, Kilbas B. Fully-automated synthesis of 177Lu labelled FAPI derivatives on the module modular lab-Eazy. *EJNMMI Radiopharm Chem.* (2021) 6:1–9. doi: 10.1186/s41181-021-00130-3
203. Jokar N, Velikyan I, Ahmadzadehfar H, Rekabpour SJ, Jafari E, Ting HH, et al. Theranostic approach in breast cancer: a treasured tailor for future oncology. *Clin Nucl Med.* (2021) 46:E410–20. doi: 10.1097/RLU.0000000000003678
204. Mansi R, Nock BA, Dalm SU, Busstra MB, van Weerden WM, Maina T. Radiolabeled bombesin analogs. *Cancers.* (2021) 13:5766. doi: 10.3390/cancers13225766
205. Patel O, Shulkes A, Baldwin GS. Gastrin-releasing peptide and cancer. *Biochim Biophys Acta Rev Cancer.* (2006) 1766:23–41. doi: 10.1016/j.bbcan.2006.01.003
206. Yang M, Gao H, Zhou Y, Ma Y, Quan Q, Lang L, et al. 18 F-labeled GRPR agonists and antagonists: a comparative study in prostate cancer imaging. *Theranostics.* (2012) 1:220–9. doi: 10.7150/thno/v01p0220
207. Baratto L, Duan H, Mäcke H, Iagaru A. Imaging the distribution of gastrin-releasing peptide receptors in cancer. *J Nucl Med.* (2020) 61:792–8. doi: 10.2967/JNUMED.119.234971

208. Baratto L, Duan H, Laudicella R, Toriihara A, Hatami N, Ferri V, et al. Physiological 68Ga-RM2 uptake in patients with biochemically recurrent prostate cancer: an atlas of semi-quantitative measurements. *Eur J Nucl Med Mol Imaging.* (2020) 47:115–22. doi: 10.1007/s00259-019-04503-4
209. Reubi JC, Wenger S, Schmuckli-Maurer J, Schaer JC, Gugger M. Bombesin receptor subtypes in human cancers: detection with the universal radioligand 125I-[D-TYR6, β-ALA11, PHE13, NLE14] bombesin(6-14). *Clin Cancer Res.* (2002) 8:1139–46.
210. Carlucci G, Kuipers A, Ananias HJK, De Paula Faria D, Dierckx RAJO, Helfrich W, et al. GRPR-selective PET imaging of prostate cancer using [18F]-lanthionine-bombesin analogs. *Peptides.* (2015) 67:45–54. doi: 10.1016/j.peptides.2015.03.004
211. Pourghiasian M, Liu Z, Pan J, Zhang Z, Colpo N, Lin KS, et al. 18F-AmBF3-MJ9: a novel radiofluorinated bombesin derivative for prostate cancer imaging. *Bioorganic Med Chem.* (2015) 23:1500–6. doi: 10.1016/j.bmc.2015.02.009
212. Morgat C, Schollhammer R, Macgrogan G, Barthe N, Vélasco V, Vimont D, et al. Comparison of the binding of the gastrin-releasing peptide receptor (GRP-R) antagonist 68 Ga-RM2 and 18 F-FDG in breast cancer samples. *PLoS ONE.* (2019) 14:e210905. doi: 10.1371/journal.pone.0210905
213. Stoykow C, Erbes T, Maecke HR, Bulla S, Bartholomä M, Mayer S, et al. Gastrin-releasing peptide receptor imaging in breast cancer using the receptor antagonist 68Ga-RM2 And PET. *Theranostics.* (2016) 6:1641–50. doi: 10.7150/thno.14958
214. Michalski K, Stoykow C, Bronsert P, Juhasz-Böss I, Meyer PT, Ruf J, et al. Association between gastrin-releasing peptide receptor expression as assessed with [68Ga]Ga-RM2 PET/CT and histopathological tumor regression after neoadjuvant chemotherapy in primary breast cancer. *Nucl Med Biol.* (2020) 86–7:37–43. doi: 10.1016/j.nucmedbio.2020.05.003
215. Michalski K, Kemna L, Asberger J, Grosu AL, Meyer PT, Ruf J, et al. Gastrin-Releasing peptide receptor antagonist [68Ga]RM2 PET/CT for staging of pre-treated, metastasized breast cancer. *Cancers.* (2021) 13:6106. doi: 10.3390/cancers13236106
216. Irelli A, Sirufo MM, Morelli L, D'ugo C, Ginaldi L, De Martinis M. Neuroendocrine cancer of the breast: a rare entity. *J Clin Med.* (2020) 9:1452. doi: 10.3390/jcm9051452
217. Tsang JY, Tse GM. Breast cancer with neuroendocrine differentiation: an update based on the latest WHO classification. *Mod Pathol.* (2021) 34:1062–73. doi: 10.1038/s41379-021-00736-7
218. Ambinder EB, Werner RA, Rowe SP. Incidental primary breast cancer detected on surveillance 68Ga-DOTATATE PET/CT in a patient with metastatic neuroendocrine carcinoma. *Radiol Case Rep.* (2020) 15:1344–7. doi: 10.1016/j.radcr.2020.05.054
219. Elgeti F, Amthauer H, Denecke T, Steffen I, Heuck F, Stelter L, et al. Incidental detection of breast cancer by 68Ga-DOTATOC-PET/CT in women suffering from neuroendocrine tumours. *NuklearMedizin.* (2008) 47:261–5. doi: 10.3413/nukmed-0185
220. Scaramuzzi G, Murgo RM, Cuttitta A, Ciuffreda L. Neuroendocrine carcinoma of the breast. Our experience and a proposal of a therapeutic algorithm for a rare tumor. *G Chir.* (2008) 29:203–6. Available online at: https://europepmc.org/article/med/18507954
221. Savelli G, Zaniboni A, Bertagna F, Bosio G, Nisa L, Rodella C, et al. Peptide Receptor Radionuclide Therapy (PRRT) in a patient affected by metastatic breast cancer with neuroendocrine differentiation. *Breast Care.* (2012) 7:408–10. doi: 10.1159/000343612
222. Wind NS, Holen I. Multidrug resistance in breast cancer: from *in vitro* models to clinical studies. *Int J Breast Cancer.* (2011) 2011:1–12. doi: 10.4061/2011/967419
223. Mairinger S, Erker T, Muller M, Langer O. PET and SPECT radiotracers to assess function and expression of ABC transporters *in vivo*. *Curr Drug Metab.* (2011) 12:774–92. doi: 10.2174/138920011798356980
224. Kurdziel KA, Kalen JD, Hirsch JI, Wilson JD, Bear HD, Logan J, et al. Human dosimetry and preliminary tumor distribution of 18F- fluoropaclitaxel in healthy volunteers and newly diagnosed breast cancer patients using PET/CT. *J Nucl Med.* (2011) 52:1339–45. doi: 10.2967/jnumed.111.091587
225. Mosayebnia M, Hajiramezanali M, Shahhosseini S. Radiolabeled peptides for molecular imaging of apoptosis. *Curr Med Chem.* (2020) 27:7064–89. doi: 10.2174/0929867327666200612152655
226. Hu S, Kiesewetter DO, Zhu L, Guo N, Gao H, Liu G, et al. Longitudinal PET imaging of doxorubicin-induced cell death with 18F-annexin v. *Mol Imaging Biol.* (2012) 14:762–70. doi: 10.1007/s11307-012-0551-5
227. Li X, Link JM, Stekhova S, Yagle KJ, Smith C, Krohn KA, et al. Site-specific labeling of annexin V with F-18 for apoptosis imaging. *Bioconjug Chem.* (2008) 19:1684–8. doi: 10.1021/bc800164d
228. Chopra A. 2-(5-[18F]Fluoro-pentyl)-2-methyl-malonic acid (ML-10). In: *Molecular Imaging and Contrast Agent Database (MICAD)*. Bethesda, MD: National Center for Biotechnology Information (2004–2013). Available online at: https://www.ncbi.nlm.nih.gov/books/NBK100897/
229. Beroske L, Van den Wyngaert T, Stroobants S, Van der Veken P, Elvas F. Molecular imaging of apoptosis: the case of caspase-3 radiotracers. *Int J Mol Sci.* (2021) 22:3948. doi: 10.3390/ijms22083948
230. Dubash SR, Merchant S, Heinzmann K, Mauri F, Lavdas I, Inglese M, et al. Clinical translation of [18F]ICMT-11 for measuring chemotherapy-induced caspase 3/7 activation in breast and lung cancer. *Eur J Nucl Med Mol Imaging.* (2018) 45:2285–99. doi: 10.1007/s00259-018-4098-9
231. Malkowski B, Wareluk P, Gorycki T, Skrobisz K, Studniarek M. Normal uptake of 11C-acetate in pancreas, liver, spleen, and suprarenal gland in PET. *Can J Gastroenterol Hepatol.* (2017) 2017:4. doi: 10.1155/2017/5478068
232. Ho CL, Cheung MK, Chen S, Cheung TT, Leung YL, Cheng KC, et al. [18F]fluoroacetate positron emission tomography for hepatocellular carcinoma and metastases: an alternative tracer for [11c]acetate? *Mol Imaging.* (2012) 11:229–39. doi: 10.2310/7290.2011.00043
233. Verwer EE, Kavanagh TR, Mischler WJ, Feng Y, Takahashi K, Wang S, et al. [18F]fluorocholine and [18F]fluoroacetate PET as imaging biomarkers to assess phosphatidylcholine and mitochondrial metabolism in preclinical models of TSC and LAM. *Clin Cancer Res.* (2018) 24:5925–38. doi: 10.1158/1078-0432.CCR-17-3693
234. Liao GJ, Clark AS, Schubert EK, Mankoff DA. 18F-fluoroestradiol PET: current status and potential future clinical applications. *J Nucl Med.* (2016) 57:1269–75. doi: 10.2967/jnumed.116.175596
235. Langbein T, Weber WA, Eiber M. Future of theranostics: an outlook on precision oncology in nuclear medicine. *J Nucl Med.* (2019) 60:13S–9S. doi: 10.2967/JNUMED.118.220566
236. Bhushan A, Gonsalves A, Menon JU. Current state of breast cancer diagnosis, treatment, and theranostics. *Pharmaceutics.* (2021) 13:723. doi: 10.3390/pharmaceutics13050723
237. Jiang M, Yang J, Li K, Liu J, Jing X, Tang M. Insights into the theranostic value of precision medicine on advanced radiotherapy to breast cancer. *Int J Med Sci.* (2021) 18:626–38. doi: 10.7150/ijms.49544
238. Bianchini G, Balko JM, Mayer IA, Sanders ME, Gianni L. Triple-negative breast cancer: challenges and opportunities of a heterogeneous disease. *Nat Rev Clin Oncol.* (2016) 13:674–90. doi: 10.1038/nrclinonc.2016.66

Conflict of Interest: The authors declare that the research was conducted in the absence of any commercial or financial relationships that could be construed as a potential conflict of interest.

Publisher's Note: All claims expressed in this article are solely those of the authors and do not necessarily represent those of their affiliated organizations, or those of the publisher, the editors and the reviewers. Any product that may be evaluated in this article, or claim that may be made by its manufacturer, is not guaranteed or endorsed by the publisher.

Copyright © 2022 Balma, Liberini, Racca, Laudicella, Bauckneht, Buschiazzo, Nicolotti, Peano, Bianchi, Albano, Quartuccio, Abgral, Morbelli, D'Alessandria, Terreno, Huellner, Papaleo and Deandreis. This is an open-access article distributed under the terms of the Creative Commons Attribution License (CC BY). The use, distribution or reproduction in other forums is permitted, provided the original author(s) and the copyright owner(s) are credited and that the original publication in this journal is cited, in accordance with accepted academic practice. No use, distribution or reproduction is permitted which does not comply with these terms.